Proteome Analysis in Arabidopsis Reveals Shoot- and Root-Specific Targets of Cytokinin Action and Differential Regulation of Hormonal Homeostasis[1][W][OA]

Markéta Žďárská[2], Pavlína Zatloukalová[2], Mariana Benítez[3], Ondrej Šedo, David Potěšil, Ondřej Novák, Jana Svačinová, Bedřich Pešek, Jiří Malbeck, Jana Vašíčková, Zbyněk Zdráhal, and Jan Hejátko*

Functional Genomics and Proteomics of Plants (M.Ž., P.Z., M.B., J.V., J.H.) and Core Facility-Proteomics (O.Š., D.P., Z.Z.), Central European Institute of Technology, Masaryk University, CZ–625 00 Brno, Czech Republic; Laboratory of Growth Regulators, Faculty of Science, Palacky University, and Institute of Experimental Botany, Academy of Sciences of the Czech Republic, CZ–783 71 Olomouc, Czech Republic (O.N., J.S.); and Laboratory of Mass Spectrometry, Institute of Experimental Botany, Academy of Sciences of the Czech Republic, CZ–165 02 Prague, Czech Republic (B.P., J.M.)

The plant hormones cytokinins (CKs) regulate multiple developmental and physiological processes in Arabidopsis (*Arabidopsis thaliana*). Responses to CKs vary in different organs and tissues (e.g. the response to CKs has been shown to be opposite in shoot and root samples). However, the tissue-specific targets of CKs and the mechanisms underlying such specificity remain largely unclear. Here, we show that the Arabidopsis proteome responds with strong tissue and time specificity to the aromatic CK 6-benzylaminopurine (BAP) and that fast posttranscriptional and/or posttranslational regulation of protein abundance is involved in the contrasting shoot and root proteome responses to BAP. We demonstrate that BAP predominantly regulates proteins involved in carbohydrate and energy metabolism in the shoot as well as protein synthesis and destination in the root. Furthermore, we found that BAP treatment affects endogenous hormonal homeostasis, again with strong tissue specificity. In the shoot, BAP up-regulates the abundance of proteins involved in abscisic acid (ABA) biosynthesis and the ABA response, whereas in the root, BAP rapidly and strongly up-regulates the majority of proteins in the ethylene biosynthetic pathway. This was further corroborated by direct measurements of hormone metabolites, showing that BAP increases ABA levels in the shoot and 1-aminocyclopropane-1-carboxylic acid, the rate-limiting precursor of ethylene biosynthesis, in the root. In support of the physiological importance of these findings, we identified the role of proteins mediating BAP-induced ethylene production, METHIONINE SYNTHASE1 and ACC OXIDASE2, in the early root growth response to BAP.

The shoot and root of Arabidopsis (*Arabidopsis thaliana*) share the expression and function of molecules crucial for organ formation and maintenance (for review, see Dinneny and Benfey, 2008; Stahl and Simon, 2010). This has led to the hypothesis that similar regulatory networks underlie comparable developmental processes in the shoot and root of Arabidopsis (Stahl and Simon, 2010). However, additional studies have indicated that the regulatory networks associated with shoot and root development also exhibit important differences, particularly in the case of hormonal regulation. Identical hormones or gene families involved in hormonal regulation may interact with tissue-specific molecules and thus can have contrasting effects on the proliferation-differentiation dynamics in each part of the plant (Kyozuka, 2007). This implies that the regulation of shoot and root developmental processes might differ more than previously thought. Thus, tissue-specific studies on hormonal action may help to clarify to what extent the respective regulatory networks in different organs and tissues are similar in terms of their components and regulatory interactions.

The plant hormones cytokinins (CKs) constitute a class of growth regulators involved in the stress response, senescence, photosynthesis, nutrient assimilation, and mobilization as well as modulation of a plant tissue's ability to act as a sink or source of metabolites (for review, see Werner and Schmülling, 2009). However, the molecular targets associated with the aforementioned processes are still largely unknown. Moreover, the CK-mediated regulation may operate differently in

[1] This work was supported by the Central European Institute of Technology project (grant no. CZ.1.05/1.1.00/02.0068), the Czech Science Foundation (grant no. P501/11/1150), and the Internal Grant Agency of Palacký University (grant nos. PrF_2012_006 and PrF_2012_016).

[2] These authors contributed equally to the article.

[3] Present address: Departamento de Ecología de la Biodiversidad, Instituto de Ecología, Universidad Nacional Autónoma de México, Apartado Postal 70-275, México City, Distrito Federal, Mexico 04510.

* Corresponding author; e-mail hejatko@sci.muni.cz.

The author responsible for distribution of materials integral to the findings presented in this article in accordance with the policy described in the Instructions for Authors (www.plantphysiol.org) is: Jan Hejátko (hejatko@sci.muni.cz).

[W] The online version of this article contains Web-only data.

[OA] Open Access articles can be viewed online without a subscription.

www.plantphysiol.org/cgi/doi/10.1104/pp.112.202853

distinct parts of the plant. For example, whereas CKs stimulate shoot apical meristem activity and size (Kurakawa et al., 2007), they act as negative regulators of the proximal root apical meristem (RAM) size, mostly via CK-induced cell differentiation (Dello Ioio et al., 2007). Thus, it is important to identify the mechanisms behind the tissue-specific regulation of CK molecular targets.

CKs are recognized by a subset of sensor His kinases, and the signal is transmitted to the nucleus via a multistep phosphorelay, thus activating the expression of target genes (for review, see Hwang et al., 2012). Previous studies have identified a wide spectrum of CK-regulated genes. CKs have been shown to modulate the expression of genes involved in the control of meristem activity, hormonal cross talk, nutrient acquisition, and various stress responses (Brenner et al., 2012). Recently, some level of shoot and root specificity was proven in the CK-mediated regulation of the transcript abundance of several genes. However, the vast majority of CK-regulated transcription was found to be similar in the shoot and root (Brenner and Schmulling, 2012). In addition to the CK-mediated regulation of transcription, several recent studies have provided growing evidence for the role of CKs in the posttranscriptional and/or posttranslational regulation of various developmental and physiological processes in Arabidopsis. CKs and CK primary response genes have been shown to regulate the stability of transporters of another plant hormone, auxin (Pernisová et al., 2009; Růžička et al., 2009; Marhavý et al., 2011; Zhang et al., 2011). CKs mediate the feedback regulation of CK signaling via CK-mediated proteolysis of B-type ARABIDOPSIS RESPONSE REGULATOR (ARR), ARR2 (Kim et al., 2012), and changes in the proteome and phosphoproteome have been shown to be part of the fast CK response in Arabidopsis (Černý et al., 2011). These findings suggest that posttranscriptional regulatory activity may indeed be a mechanism involved in the contrasting behavior and response of the different plant tissues. Thus, in order to study the origin of CK tissue specificity and the nature of hormonal cross talk in different plant organs and tissues, it is important to identify proteins under CK control at a posttranscriptional and/or posttranslational level in a tissue-specific manner. Moreover, whole-genome transcriptomic data sets are now widely available (Rashotte et al., 2003; Brenner et al., 2005; Brenner and Schmulling, 2012), which can be complemented and compared with proteomic studies. This should help to elucidate the relative contributions of both types of regulation during plant development.

In this study, we analyzed 6-benzylaminopurine (BAP)-mediated proteome regulation specifically in the shoot and root of Arabidopsis. We showed that the proteome response to BAP has a strong tissue and time specificity and identified targets of BAP-mediated regulation. In particular, the results revealed that the tissue-specific regulation of hormonal homeostasis is an intrinsic feature of the BAP response. These findings contribute to our understanding of how the regulatory interactions among similar molecules can be modified in a tissue-specific manner and provide a plausible explanation for one of the possible mechanisms behind the long known shoot and root specificity of the CK response in plants.

RESULTS

BAP Uptake Is Comparable in the Shoot and Root

We analyzed the time and tissue specificity of the CK response in 6-d-old seedlings treated with exogenous 5 μM BAP separately in the shoot and root for two different time intervals: 30 min (hereafter referred to as the "early" response) and 120 min of incubation (hereafter referred to as the "delayed" BAP response; designations were according to Brenner et al. [2005]). To ensure that the applied BAP passed through the environmental barrier and conveyed to the examined tissues, we measured the levels of BAP in both tissues and for both time intervals. We did not detect any BAP in mock-treated controls, as expected, but observed similar BAP levels in the BAP-treated shoots and roots (Fig. 1). Although surface-bound BAP might partially distort the measurements, a slight increase in BAP levels following the 120-min treatment, in contrast to the 30-min treatment, indicated that we predominantly measured internally accumulated BAP. Furthermore, levels of metabolized BAP (hydroxylated BAP derivatives, *ortho*- and *para*-topolin) showed a similar response in both tissues following the 30-min treatment, whereas after the 120-min treatment, we observed slightly higher levels in the shoot samples than in the

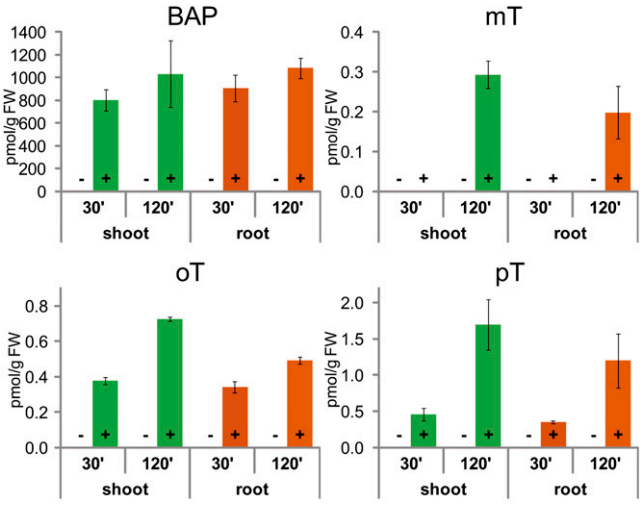

Figure 1. Comparable BAP uptake in shoot and root samples. Levels of BAP and hydroxylated BAP derivatives (*meta*-, *ortho*-, and *para*-topolin, denoted mT, oT, and pT, respectively) were measured in the mock-treated (DMSO) and BAP-treated (5 μM) samples (denoted by – and +, respectively). The measurements were performed in three independent biological replicates. Error bars show SD. FW, Fresh weight.

root samples (Fig. 1). Overall, these results indicated similar BAP uptake by the shoot and root, as suggested by the direct measurements of BAP and its metabolic products.

BAP Induces Time- and Tissue-Specific Proteome Changes in Arabidopsis

In order to understand the molecular mechanisms behind the BAP response at the protein level, we analyzed the proteome of BAP-treated seedlings. We used two-dimensional gel electrophoresis with fluorescent Sypro Ruby gel staining of both shoot and root samples treated with BAP for the above-mentioned time intervals. Image analysis of the two-dimensional gels (four biological replicas) revealed qualitative (presence or absence of the respective spot) and quantitative changes in the protein abundance in comparison with the mock-treated controls. Individual proteins with changed expression were identified by liquid chromatography-tandem mass spectrometry (for a detailed description of the assay, see "Materials and Methods"). On average, 1,900 protein spots were monitored on gels obtained from shoot isolates, whereas around 1,500 protein spots were detected on gels corresponding to root isolates. Overall, we identified 43/18 (early/delayed response) differentially regulated proteins in the shoot and 31/21 differentially regulated proteins in the root. We classified the proteins according to their type of response and time specificity (Fig. 2); for a complete list, see Supplemental Table S1.

Unexpectedly, we found only one protein regulated by BAP in both tissues (AT4G14880, AtCYS-3A/OASA1/OLD3), which suggests the high tissue specificity of the Arabidopsis response to BAP. Considering the time specificity, only two proteins in the shoot, AT4G20360 (Rab GTPase homolog E1B) and ATCG00490 (large subunit of Rubisco [RBCL]), were identified as BAP regulated for both time intervals (both proteins were up-regulated at the early time point and down-regulated at the delayed time point; Supplemental Table S1). In the root, we did not identify any proteins regulated by BAP in both time intervals.

Thus, following BAP treatment, we observed mostly shoot- and root-specific proteome changes that also depended on the time point.

BAP Regulates Carbohydrate and Energy Metabolism in the Shoot

To gain an insight into the biological role of the BAP-regulated proteins in both tissues, we categorized the BAP-regulated proteins according to the classification introduced by Bevan et al. (1998) and mapped the proteins in the annotated pathway maps provided by the Kyoto Encyclopedia of Genes and Genomes (KEGG; http://www.genome.jp/kegg/). We were able to map 68 of the 104 proteins (65%) identified in this study (Supplemental Figs. S1 and S2; Supplemental Tables S1

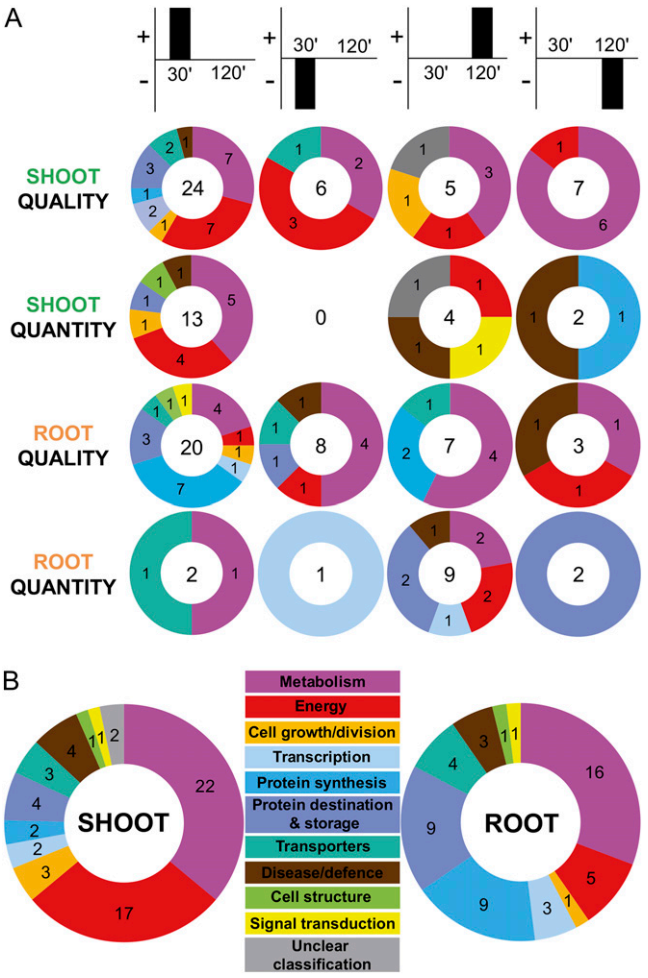

Figure 2. BAP application induces specific proteome changes in the shoot and root. A, Classification of BAP-regulated proteins according to the type of response and its tissue and time specificity. Qualitative (presence or absence of the protein in comparison with the mock-treated control) and statistically significant changes in the protein abundance (Student's *t* test; four biological replicates) were evaluated separately for both tissues and assayed time intervals. The number inside the chart shows the total number of identified proteins in each category. B, Functional distribution of proteins (both up- and down-regulated) by BAP in shoot and root samples. The color code represents the functional classification according to Bevan et al. (1998).

and S2). Protein classification according to the functional categories of Bevan et al. (1998) revealed that the major portion of BAP-regulated proteins (both up- and down-regulated) in both tissues were proteins involved in processing metabolites of different pathways, such as amino acid, nitrogen, nucleotide, sugar, and lipid metabolism (Fig. 2B).

In the shoot, the second major class of BAP-regulated proteins contained proteins involved in energy-associated (energy acquisition or storage) processes, such as glycolysis, gluconeogenesis, and photosynthesis. Accordingly, using the KEGG database, we mapped most of the BAP-regulated proteins in the shoot to carbohydrate metabolism and energy acquisition (Supplemental Fig.

S1A; Supplemental Table S2). The roles of these proteins have been annotated in basic metabolic pathways, including starch and Suc metabolism, glycolysis, and gluconeogenesis (Supplemental Fig. S1B), pyruvate metabolism (Supplemental Fig. S1C), carbon fixation (Supplemental Fig. S1D), citrate cycle (Supplemental Fig. S1E), and oxidative phosphorylation, photosynthesis, and chlorophyll metabolism (Supplemental Table S2). Shoot-identified proteins that were not mapped but have previously been described in the literature also indicate CK control over protein import in chloroplasts (AT5G16620, PDE120/ATTIC40; Bédard et al., 2007) or control of meristem size via correct folding and/or complex formation of CLV proteins (AT4G24190, SHD/AtHSP90.7; Ishiguro et al., 2002).

With regard to the time specificity of the shoot response, most of the aforementioned processes were found to be predominantly regulated at the early-response time point, except for purine, porphyrin, and chlorophyll metabolism, which were found to be regulated during the delayed response (Supplemental Fig. S1).

BAP Targets Protein Synthesis and Destination in the Root

As in the shoot, the most abundant category of proteins regulated by BAP in the root related to metabolism. However, in contrast to the shoot response, the second most represented category in the root constituted proteins involved in protein destination and storage, such as protein folding, targeting, modification, and proteolysis. At the same frequency, BAP regulated proteins in the root associated with protein synthesis, like ribosomal proteins and tRNA synthases (Fig. 2B). With respect to KEGG mapped pathways, one of the most affected processes in the root was RNA transport (Supplemental Fig. S2A). Four of the BAP-regulated proteins have been annotated as proteasome components, three of which we identified in the root (Supplemental Fig. S2B). Several other BAP-regulated proteins in the root have been annotated as proteins involved in the proteasome-mediated regulation of protein stability (AT1G16190, AT5G22610), in protein folding (AT3G03960, AT3G18190), or in protein processing in the endoplasmic reticulum (ER; Supplemental Fig. S2C). Regarding metabolic processes, proteins involved in amino sugar and nucleotide sugar metabolism (Supplemental Fig. S2D), as well as Cys and Met metabolism (Supplemental Fig. S2E), were also found to be predominantly regulated in the root. This suggests a role for BAP in regulating Met-related metabolism in the root (see below). Previously characterized nonmapped proteins connect BAP action in the root with, for example, the organization of cortical microtubule arrays and cellular patterning (AT3G55000, TONNEAU1; Azimzadeh et al., 2008) or the regulation of telomere-length homeostasis and salicylic acid-dependent disease resistance (AT1G14410, ATWHY1/PTAC1; Desveaux et al., 2004; Yoo et al., 2007). This is consistent with recently published data on CK cross talk with the salicylic acid-mediated immune response (Choi et al., 2010; Argueso et al., 2012).

Similar to the shoot, most of the BAP-regulated proteins in the root were found to be differentially regulated during the early response, except for proteasome-mediated protein degradation or amino sugar and nucleotide sugar metabolism, which were mainly targeted during the delayed response (Supplemental Table S2).

In both shoot and root, we found a substantial proportion of BAP-regulated proteins to be stress related, including those involved in ascorbate metabolism (Supplemental Fig. S1F; Supplemental Table S1) and others related to the cold or heat response (Supplemental Table S1).

Altogether, our results imply that the proteome response to BAP in Arabidopsis is tissue and time specific. The BAP-mediated proteome regulation appears to be important, particularly as an immediate regulatory mechanism, because of the higher number of differentially regulated proteins during the early response in both assayed tissues. Mapping the annotated activities of the identified proteins suggested a predominant role for BAP-mediated regulation in carbohydrate and energy metabolism within the shoot and in protein synthesis and protein processing within the root.

BAP-Mediated Proteome Regulation Occurs Dominantly at the Posttranscriptional and/or Posttranslational Level

CKs have been identified as effective regulators of gene transcriptional activity. Thus, we wanted to identify the contribution of CK-mediated transcriptional regulation to the observed proteome response. Therefore, we selected a subset of BAP-modulated proteins from our data set, in particular, proteins covering the two tissues and time points whose function had already been described. We analyzed BAP-mediated changes in the abundance of 21 mRNAs using quantitative real-time PCR. Two out of the 11 genes assayed in the shoot and two out of 10 in the root exhibited the same type of response as their protein products, whereas nine out of 11 genes in the shoot and eight out of 10 in the root displayed no statistically significant transcriptional response (Fig. 3, A and B). This agrees well with the results of previously performed transcriptional studies (Rashotte et al., 2003; Brenner et al., 2005; Brenner and Schmulling, 2012), demonstrating only minimal or no overlap with our proteome data set (data not shown). In the case of AtPHB3, one of the proteins exhibiting no transcriptional response, the posttranscriptional and/or posttranslational nature of BAP-mediated regulation was confirmed by immunostaining (Fig. 3C).

Overall, our results demonstrate only limited overlap between regulation at the transcript and protein abundance levels and suggest a substantial role for post-transcriptional and/or posttranslational regulation in the proteome response to BAP.

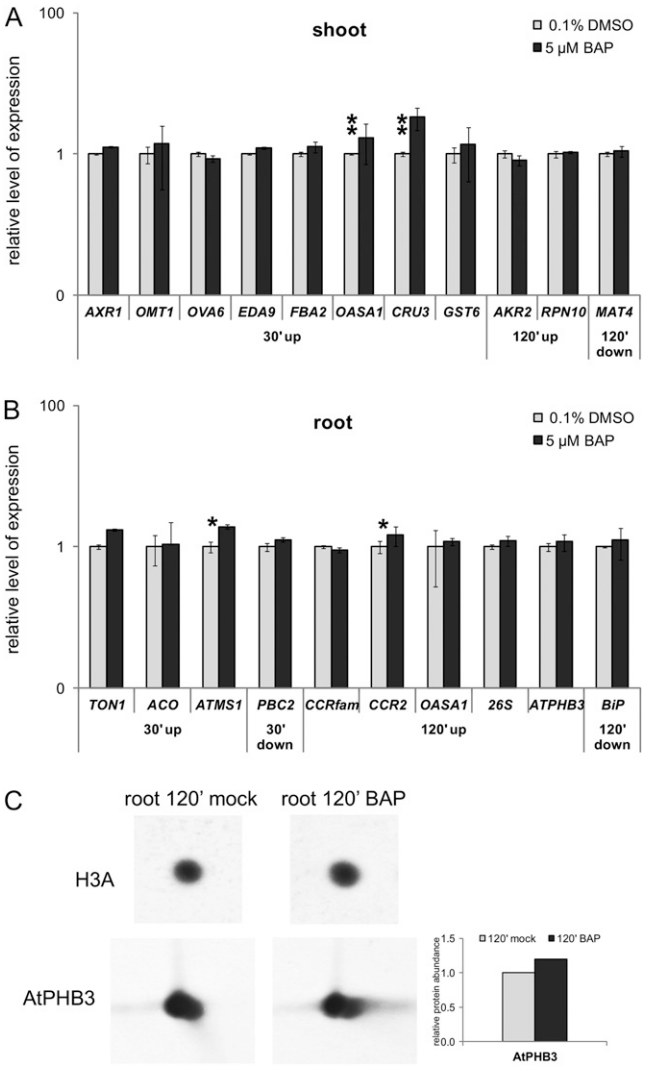

Figure 3. Comparison of the transcriptional type of regulation with the proteome response. A and B, BAP responses of selected genes encoding proteins revealing BAP-mediated changes in the shoot (A) and root (B); note logarithmical scale of the *y* axes. The statistical significance of differences between mock-treated (−) and BAP-treated (+) samples (Student's *t* test) at $\alpha = 0.05$ and 0.01 is denoted by single and double asterisks, respectively. Error bars indicate SD. C, A 1.2-fold increase in AtPHB3 abundance was detected in the independent isolation by immunodetection using AtPHB3 antibodies compared with a 1.5-fold increase identified by Sypro Ruby staining. The histone H3A antibody was used as an internal control for total protein amount normalization.

BAP Regulates Proteins Involved in Hormonal Metabolism

In our proteomic analysis, we detected several BAP-regulated proteins that were mapped in diverse steps of plant hormone biosynthesis (Fig. 4; Supplemental Fig. S4). In general, we found that modulation of the ethylene biosynthetic pathway was the most prominent. Ethylene is biosynthesized in four catalytic steps, and it has been shown previously that CKs stabilize ACC SYNTHASE (Chae et al., 2003; Hansen et al., 2009), catalyzing the third step in this pathway. Here, we identified that all three remaining enzymes of the ethylene biosynthetic pathway were up-regulated by BAP: MET SYNTHASE1 (AtMS1; AT5G17920), MET ADENOSYLTRANSFERASE3 (MAT3; AT2G36880), and

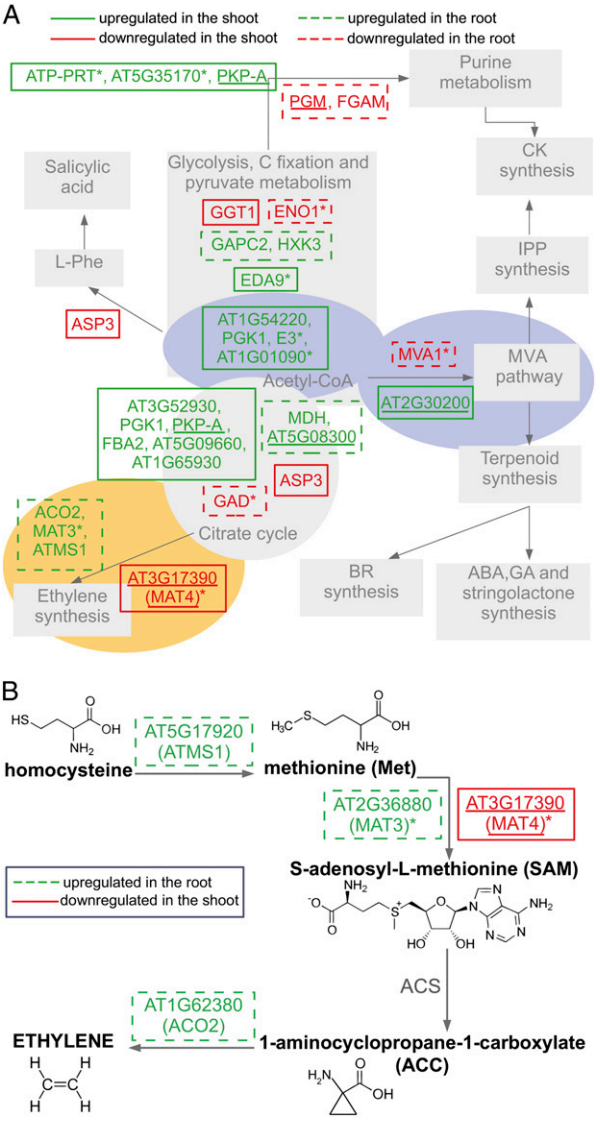

Figure 4. BAP regulates endogenous hormone metabolism specifically in the shoot and root. A, Overview of BAP-regulated proteins participating in the metabolism of endogenous hormones. Proteins involved in the MVA pathway and ethylene biosynthesis are highlighted as blue and orange ovals, respectively. B, BAP tightly regulates ethylene biosynthesis in the root. In addition to the enzymes identified as up-regulated by BAP in our study, CK-mediated stabilization of a subset of ACS has been demonstrated previously (Chae et al., 2003; Hansen et al., 2009). In both A and B, proteins regulated in the root are framed within dashed lines, whereas those regulated in the shoot are framed within continuous lines. Down-regulated proteins are shown in red, and up-regulated genes are shown in green. Proteins regulated after 120 min are underlined. PKP-A, pyruvate kinase; PGM, glucose phosphomutase, putative; FGAM, phosphoribosylformylglycinamidine synthase; IPP, isopentenyl pyrophosphate; GAD, Glu decarboxylase; BR, brassinosteroid.

ACC OXIDASE2 (ACO2; AT1G62380; Fig. 4B). Importantly, we found that the enzymes were up-regulated specifically during the early response of the root, indicating that BAP-mediated up-regulation of ethylene biosynthesis is very fast and tissue specific. It is worth noting that we identified another MAT isoform, MAT4, that was down-regulated in the delayed shoot response, thus further contrasting the tissue-specific BAP regulation of the ethylene biosynthetic pathway (Supplemental Fig. S3; Supplemental Table S1). Furthermore, in the case of AtMS1, we found that the BAP-mediated up-regulation occurs at the transcriptional level (Fig. 3B).

Besides ethylene biosynthesis, we found that BAP regulates proteins belonging to the mevalonate acid (MVA) pathway, namely AT2G30200 (EMB3147) and AT4G11820 (MVA1; Fig. 4A). This pathway is generally important in hormone biosynthesis; it is crucial for brassinosteroid synthesis and is also involved in the biosynthesis of gibberellin (Kasahara et al., 2002), CKs (Kasahara et al., 2004), and possibly abscisic acid (ABA; Milborrow, 2001; Fig. 2A; Supplemental Fig. S3). Importantly, we found that the aforementioned proteins of the MVA pathway are regulated in a tissue-specific way: positive in the shoot and negative in the root (Fig. 4A; Supplemental Fig. S3; Supplemental Table S1). Also, acetyl-CoA production, which is a key metabolite initiating the MVA pathway, seems to be under strong positive control by BAP during the early response of the shoot (Supplemental Figs. S1, B and E, and S3). In agreement with this, we found several ABA-related proteins to be CK regulated predominantly in the shoot. Among the nine ABA-related proteins found in our data set, seven were identified in the shoot, five of which were up-regulated in the early shoot response (Supplemental Table S3). Three (RBCL, FBA2, and CRU3/CRC) have been shown to be Tyr phosphorylated in response to ABA (Ghelis et al., 2008), and transcription of *AtCYS-3A/OASA1/OLD3* is reportedly increased by ABA (Barroso et al., 1999). In agreement, we observed both up-regulation of *AtCYS-3A/OASA1/OLD3* in the shoots of CK-treated seedlings and also that *CRU3* was under distinctive CK-mediated transcriptional control during the early shoot response (Supplemental Fig. S3A).

Besides ethylene- and ABA-related proteins, we also identified several BAP-regulated proteins that are potentially associated with CK biosynthesis (Supplemental Fig. S3). Specifically, AT1G58080, AT3G22960, and AT5G35170 regulate the production of AMP, ADP, and ATP (Supplemental Fig. S3; Supplemental Table S2), which are substrates of adenosine phosphate-isopentenyltransferases in the first step of CK biosynthesis. This is consistent with previously published data showing that CKs can regulate their own biosynthesis (Sakakibara et al., 2006, and refs. therein).

Taken together, our results show that BAP regulates several proteins involved in hormone biosynthesis or associated with hormone-mediated regulation and that BAP modulation of hormonal regulation exhibits significant tissue specificity. We identified strong, rapid up-regulation of proteins catalyzing ethylene biosynthesis in the root and up-regulation of the MVA pathway and several ABA-related proteins mainly in the shoot.

BAP Treatment Affects the Tissue-Specific Distribution of Endogenous Hormones

Results of our proteomic analysis suggested potential tissue-specific cross talk between CKs and the biosynthesis or action of other phytohormones. Therefore, we examined the BAP-mediated changes in endogenous levels of 1-aminocyclopropane-1-carboxylic acid (ACC), the rate-limiting precursor of ethylene biosynthesis, ABA, and endogenous CKs and their metabolites, again for both inspected tissues and time points.

ACC distribution and its CK-dependent regulation revealed remarkable tissue specificity. In untreated controls, levels of ACC in the root were below the detection limit but increased substantially upon CK application. By contrast, levels of ACC in the shoot were almost unaffected by CK treatment (Fig. 5A). The root-specific increase in ethylene production was further confirmed by the staining of the ethylene-responsive reporter line carrying GUS under the control of four synthetic copies of the EIN3-binding site (EBS; Solano et al., 1998; Supplemental Fig. S7). This is notably in agreement with our results suggesting tight CK-mediated control over ethylene biosynthesis specifically in the root (Fig. 4B). In the case of ABA, we detected slightly higher levels in mock-treated roots than shoots. Following BAP treatment, we found significant up-regulation of ABA levels, particularly in the early response of the shoot (Fig. 5A). In the root, we identified a slight (statistically insignificant) decrease in the ABA amount for both time points. These ABA measurements corroborate with the positive BAP regulation of the MVA pathway and with acetyl-CoA biosynthesis in the shoot and negative regulation of the MVA pathway in the root (Supplemental Figs. S1E and S3).

Endogenous levels of the free CK bases trans-zeatin (tZ), isopentenyladenine (iP), and cis-zeatin (cZ) also displayed strong tissue specificity (Fig. 5B), which was most pronounced in the case of cZ. The amount of cZ in the root was approximately 10 times higher than the amount detected in the shoot. BAP treatment even enhanced the asymmetric distribution of cZ during the delayed response, leading to its down-regulation in the shoot and up-regulation in the root (Fig. 5B). Furthermore, we noticed that cZ was the dominant CK in the root, with levels six to 10 times higher than for tZ. This cZ dominance was even more apparent in the case of CK nucleosides, where we found about 15 to 185 and 15 to 40 times higher levels of cZ riboside in comparison with tZ riboside and iP riboside, respectively (Supplemental Fig. S4). Interestingly, as for cZ, an asymmetry favoring root accumulation was

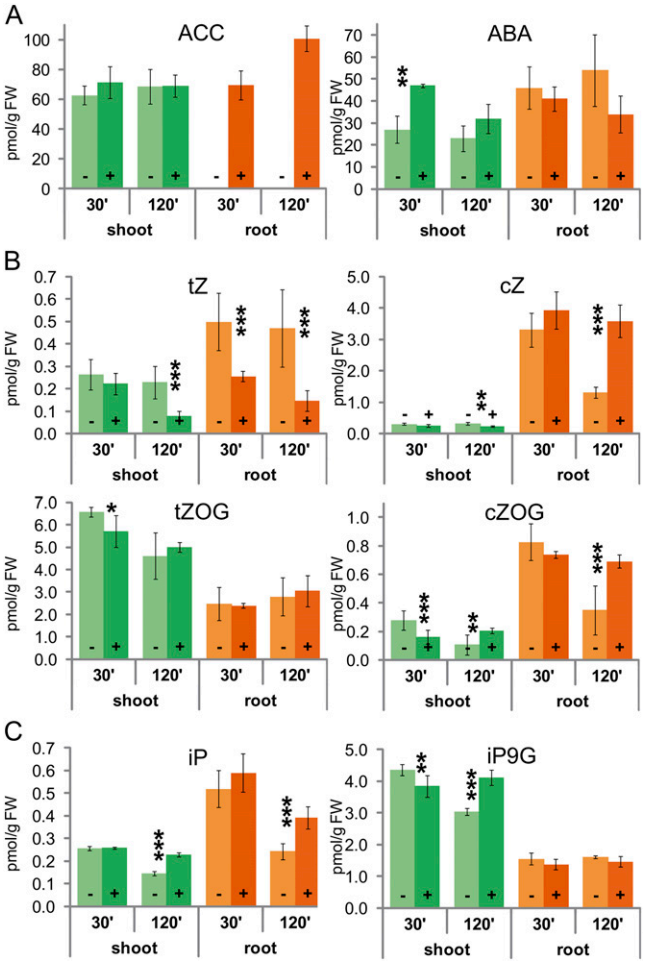

Figure 5. Exogenous BAP application affects levels of endogenous hormones and their metabolites differentially in the shoot and root. A, Root- and shoot-specific changes of ACC and ABA levels, respectively. B and C, Endogenous CKs and their metabolites exhibit tissue-specific distributions and responses to exogenous BAP. The statistical significance of differences between mock-treated (−) and BAP-treated (+) samples (Student's *t* test) at $\alpha = 0.05$, 0.01, and 0.001 is denoted by single, double, and triple asterisks, respectively. Error bars indicate SD. cZOG, Cis-zeatin-*O*-glucoside; FW, fresh weight; iP9G, isopentenyladenide-*N*9-glucoside; tZOG, trans-zeatin-*O*-glucoside.

detected for dihydrozeatin riboside but not for tZ riboside. For iP and tZ, a consistent type of regulation was found in both tissues and time intervals assayed, whereas opposing types of responses were observed for both CK types: While the levels of tZ significantly decreased in both tissues upon the addition of BAP, iP was slightly up-regulated or not affected by BAP in both root and shoot (Supplemental Fig. S2, B and C, respectively).

Collectively, these results agree with our proteomic data suggesting tissue-specific BAP-mediated hormonal cross talk. Our results provide experimental evidence for tight BAP-mediated control of ethylene biosynthesis in the root and ABA biosynthesis in the shoot. The significant tissue specificity is also apparent in the distribution of endogenous CKs as well as in the BAP-mediated regulation of endogenous CK metabolism.

Proteins Catalyzing BAP-Induced Ethylene Biosynthesis Mediate the Root Response to BAP

The roles of both CK and ethylene in mediating root shortening have been described (Cary et al., 1995; Růžička et al., 2007). Our proteomic analysis identified that three enzymes catalyzing the ethylene biosynthetic pathway are promptly up-regulated by BAP specifically in the root. This implies that BAP-induced ethylene may contribute to the immediate root growth response via tight control over ethylene production. To test this, we examined BAP-induced root shortening of mutants in the *ATMS1* and *ACO2* genes, encoding the first and last proteins of the ethylene biosynthetic pathway (Fig. 4B). To approximate the physiological assay to the early CK response, as studied in our proteome analysis, we employed the "seedling transfer" assay, where 6-d-old seedlings were grown on pure Murashige and Skoog (MS) medium and then transferred to MS medium supplemented with BAP and cultivated for a further 2 d. In close agreement with our model, both *atms1* and *aco2* mutants exhibited higher resistance to BAP-induced root shortening than the wild type. This effect was apparent by only day 1 after transplanting the seedlings from pure MS medium to medium supplemented with BAP (Fig. 6A). Furthermore, we compared these results with those for a mutation in the gene encoding ACS9, which has previously been shown to be stabilized by CKs (Hansen et al., 2009). Interestingly, *acs9* did not display any significant changes in root growth during day 1 of BAP incubation, and differences were only apparent after 2 d of growth in the presence of BAP (Fig. 6A). This agrees well with the lack of ASC9 stabilization by BAP in our experimental system.

CKs have been shown to control root growth via regulation of the RAM size (Dello Ioio et al., 2007; Růžička et al., 2009), whereas ethylene is reported to act specifically on the regulation of cell elongation (Růžička et al., 2007). Thus, to elucidate the mechanism of the observed influence of ethylene biosynthesis on the CK-mediated root shortening, we examined the effects of BAP on the RAM size and cell elongation in the wild type and ethylene biosynthetic mutants. Surprisingly, we found that both *atms1* and *aco2* lines exhibited resistance to the BAP-mediated reduction of RAM. However, this was not the case in the *acs9* line (Fig. 6B). In our seedling transfer assay, we were unable to detect any reduction in the elongation of cells leaving the RAM in the BAP-treated wild type and *acs9* mutants. In contrast, we observed a large reduction in root cell elongation in *atms1* and a smaller but still distinct reduction in the *aco2* line (Fig. 6B). Notably, the mock-treated *atms1* mutant had longer cells leaving the RAM than the wild type (Supplemental Fig. S6).

Altogether, these findings correlate well with our proteomic data, suggesting that BAP rapidly up-regulates

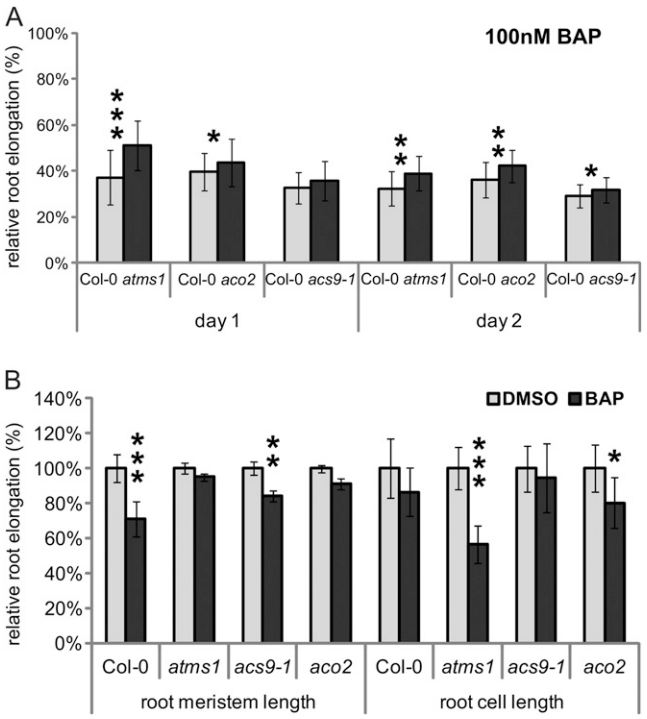

Figure 6. Relative root lengths of mutants in ethylene biosynthesis in response to BAP. Col-0 (always grown on the same plate) is shown in comparison with all mutants to demonstrate the SD used in Student's *t* test calculations. A value of 100% corresponds to the root length of the respective mock-treated controls (mean ± SD). The relative root lengths are given as follows: 4.33 ± 0.58, 4.27 ± 0.81, and 4.77 ± 0.65 mm (day 1; Col-0 controls to *atms1*, *aco2*, and *acs9-1*, respectively) and 10.82 ± 1.10, 9.68 ± 1.45, and 10.38 ± 1.05 mm (day 2; Col-0 controls to *atms1*, *aco2*, and *acs9-1*, respectively); for *atms1*, 4.95 ± 1.17 mm (day 1) and 11.64 ± 1.83 mm (day 2); for *aco2*, 4.67 ± 0.54 mm (day 1) and 10.34 ± 0.89 mm (day 2); for *acs9-1*, 5.93 ± 0.93 mm (day 1) and 13.11 ± 1.42 mm (day 2). B, Relative root meristem lengths and lengths of cells that just left the transition zone of 100 nM BAP-treated plants in comparison with mock-treated plants (2 d of incubation); the absolute values are shown in Supplemental Figure S6. The statistical significance of differences between Col-0 and the mutant lines following 100 nM BAP application (Student's *t* test) at $\alpha = 0.05$, 0.01, and 0.001 is denoted by single, double, and triple asterisks, respectively.

several members of the ethylene biosynthetic pathway that cause root-specific ACC production and interfere with the BAP effect on root growth (Fig. 7). Our data also provide evidence for the unexpected role of ethylene biosynthesis in the BAP-mediated reduction of the RAM size.

DISCUSSION

BAP-Mediated Proteome Changes Reveal Root- and Shoot-Specific Targets of CK Action

Here, we identified a set of proteins that respond to BAP application in a tissue- and time-specific manner. In the shoot, the identification of BAP-mediated control over proteins that are potentially involved in the regulation of basic metabolic processes, such as carbon fixation and chlorophyll, Suc, and starch metabolism, provides a molecular link to the previously shown CK-mediated regulation of photosynthesis (Wareing et al., 1968), chloroplast biogenesis (Reski, 1994), chlorophyll metabolism (Mok, 1994), and sink and source strength of plant tissues (Werner et al., 2008).

In the root, the processes mainly affected by BAP include the regulation of protein synthesis and destination, protein processing in the ER, and proteasome-mediated degradation. This supports recent evidence suggesting that CKs have an important role in protein targeting and proteasome-mediated protein stability. CK-induced internalization of the auxin transporter PIN1 during de novo organogenesis has been reported (Pernisová et al., 2009). CKs have been suggested to regulate the stability of diverse PIN proteins (Růžička et al., 2009; Zhang et al., 2011) and vacuolar targeting of PIN1 (Marhavý et al., 2011). The 26S proteasome subunit RPN12 has been implicated in sensitivity to CKs (Smalle et al., 2002), potentially regulating CK signaling via the stabilization of ARR5 (Ryu et al., 2009). The type-B response regulator ARR2 has also recently been found to be under the control of the 26S proteasome (Kim et al., 2012). In addition, the 26S proteasome regulatory subunit RPN10 was proposed to mediate the degradation of CK and/or auxin response repressors in *Physcomitrella patens* (Fu et al., 1999). Indeed, we found both core (20S) and regulatory subunits of the 26S proteasome to be under CK control (Supplemental Fig. S2B), suggesting potential feedback in the CK signaling via CK-mediated regulation of the 26S proteasome activity. Finally, recently identified localization of CK receptors in

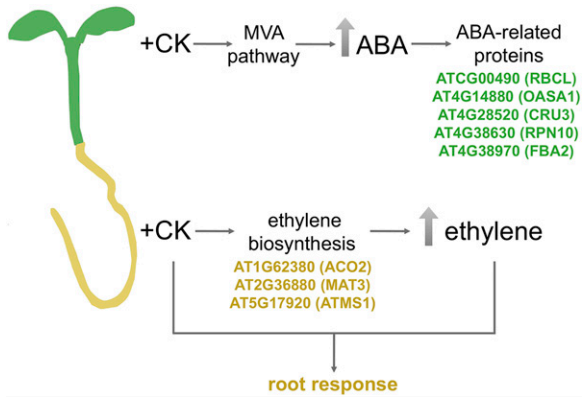

Figure 7. Schematic and simplified representation of shoot- and root-specific regulation of proteins regulating hormonal metabolism. In the shoot, BAP application up-regulates ABA levels, probably via up-regulation of proteins involved in the mevalonate pathway and acetyl-CoA formation. This leads to up-regulation of several ABA-related proteins predominantly in the shoot, potentially via Tyr phosphorylation-mediated protein stabilization or other type of ABA-dependent regulation of expression. In the root, BAP treatment up-regulates several proteins involved in ethylene biosynthesis, resulting in rapid ethylene up-regulation as a result of root-specific ACC accumulation. Both CK and ethylene are involved in the root growth response.

the ER (Caesar et al., 2011; Wulfetange et al., 2011) supports our results suggesting CK control over protein processing in the ER.

Taken together, our data reveal several novel regulators influenced by BAP in a tissue-specific way that may be potential molecular targets of the CK-mediated regulation of several processes previously identified to be under CK control.

Nontranscriptional Regulations Are Involved in the Proteome Response to BAP

The proteins identified in this study as BAP regulated showed little or no overlap with transcripts that have been previously identified as CK regulated (Rashotte et al., 2003; Brenner et al., 2005), including a recently published study on the shoot- and root-specific transcriptional profiling of CK action in Arabidopsis (Brenner and Schmulling, 2012). These results are consistent with several reports showing little or no correlation between transcript and protein levels at a given time point in several model organisms and experimental setups (Foss et al., 2007; Fu et al., 2009; Taniguchi et al., 2010; Ghazalpour et al., 2011; Ning et al., 2012). Differences in mRNA and protein lifetimes and/or extrinsic translational noise or regulatory networks may account for the observed differences in regulation at the transcript and protein levels (Fu et al., 2009; Taniguchi et al., 2010).

Accordingly, in the subset of proteins that we found to be regulated by BAP, we observed corresponding changes of the respective transcripts in only a minor (approximately 20%) fraction (Fig. 3). This clearly suggests the involvement of posttranscriptional and/or posttranslational regulation in the tissue-specific BAP regulation of the Arabidopsis proteome and implies that the transcriptional and nontranscriptional regulation of protein abundance might be rather complementary. Nevertheless, further studies are required to perform a statistical comparison of the transcript and protein abundance for different treatments as well as to search for long-term spatiotemporal correlations, both at the cell and tissue levels. The observed BAP-mediated regulation of proteins involved in RNA transport, initiation of translation, or protein degradation, as evident in our data set (Supplemental Fig. S2, A and B), revealed potential BAP targets for this type of regulation. However, identification of the molecular mechanisms underlying the BAP-mediated control over protein abundance remains a considerable challenge for future work.

BAP Affects Endogenous Hormone Levels Specifically in the Shoot and Root

Importantly, we also obtained experimental evidence that differential proteome responses underlie the shoot- and root-specific BAP regulation of hormone biosynthesis, the clearest example being the regulation of ethylene production. Our data show that BAP mediates very fast up-regulation of the ethylene biosynthetic pathway, resulting in ACC accumulation specifically in the root. It is noteworthy that we did not observe the previously reported CK-mediated stabilization of ACC synthases, neither ACS5 nor ACS9 (Chae et al., 2003; Hansen et al., 2009), possibly due to a lower detection limit or the different experimental design of our system. This is in a good agreement with our physiological analysis, suggesting that in comparison with ATMS1 and ACO2, ACS9 appears to play a relatively minor role in the early root growth response to BAP (see below). In our study, however, all three remaining enzymes of the ethylene biosynthetic pathway, AtMS1, MAT3, and ACO2, were up-regulated by BAP in the root, indicating their crucial role in the early BAP response (Fig. 7). These results are complemented and supported by a recent study on ethylene-mediated proteome changes. Among eight proteins identified to be regulated by both BAP (this study) and ethylene (Chen et al., 2011), five were identified as BAP regulated in the root (Supplemental Table S4). Nevertheless, despite the fact that the root-specific response at the level of ACC biosynthesis predominated under our experimental conditions, the involvement of a cell type-specific, ethylene-associated CK response in the delayed developmental regulation of the shoot cannot be excluded, as reported previously (Cary et al., 1995; Tanaka et al., 2006).

The observed up-regulation of ABA-related proteins in the shoot might be a consequence of the CK-mediated up-regulation of the MVA pathway and increase of ABA levels in the early shoot response (Fig. 7). Although it has been reported that the methyl erythritol phosphate pathway in chloroplasts constitutes the main branch of the ABA biosynthetic pathway, the chloroplast import of cytoplasmic isopenthenyl diphosphate produced via the MVA pathway still seems to contribute to ABA production (for review, see Milborrow, 2001). Thus, in addition to the recently reported positive role of CKs in the regulation of ABA biosynthesis at the transcriptional level (Nishiyama et al., 2011), proteome regulation by CKs could represent another mechanism of CK and ABA cross talk. The BAP-mediated up-regulation of proteins that are Tyr phosphorylated in response to ABA suggests that this type of posttranslational modification might have a stabilizing effect. This, however, remains to be clarified.

We also identified a strong asymmetry in the distribution and response of endogenous CKs and their metabolites. The most pronounced asymmetry was observed in the case of cZ and its ribosides, which we found to be the predominant CK in Arabidopsis root. Indeed, slightly higher concentrations of cZ than tZ have previously been found in the roots of hop (*Humulus lupulus*; Watanabe et al., 1982) and maize (*Zea mays*; Veach et al., 2003; Saleem et al., 2010). This tissue-specific distribution probably did not play an important role under our experimental conditions due to the relatively high concentration of exogenously applied

BAP (compare CK levels in Figs. 1 and 5). However, the recently identified specificity of the CK-degrading enzymes cytokinin oxidases/dehydrogenases (CKX; Gajdošová et al., 2011) and the diverse ability among CK types, including cZ, to bind individual CK receptors suggest that this asymmetrical distribution might indicate a potential functional importance in CK-mediated developmental control. This is further supported by our findings demonstrating the higher root accumulation of dihydrozeatin riboside. Dihydrozeatin and its derivatives are not substrates for CK degradation by CKX (Sakakibara, 2010) but are still able to activate CK signaling via AHK3 (Spíchal et al., 2004), providing further evidence for the potential tissue specificity of CKX-mediated developmental regulation, in agreement with previous observations (Werner et al., 2003).

Ethylene Biosynthesis Is Involved in the Early Root Growth Response to BAP

Root growth is regulated at the level of mitotic activity of the cells in the RAM, cell differentiation of the meristematic cells leaving the RAM in the transition zone, and elongation of cells that undergo differentiation outside the RAM. These events are integrated, with the balance between cell division and cell differentiation determining the RAM size (Dello Ioio et al., 2007). In particular, CKs have been shown to reduce RAM size via the activation of cell differentiation in the transition zone (Dello Ioio et al., 2007). Using ethylene signaling mutants, this CK effect has been suggested to be ethylene independent (Růžička et al., 2009). However, this was observed in Arabidopsis seedlings germinated and grown on medium supplemented with BAP. In our short-term experimental system via transplanting the seedlings from pure MS medium to medium supplemented with BAP, we have shown that both *atms1* and *aco2* mutants exhibit resistance to the BAP-mediated shortening of the RAM. This rather surprising finding suggests that both ATMS1 and ACO2 are necessary for the immediate root growth response at the level of BAP-mediated regulation of RAM size. Nevertheless, further detailed analysis will be necessary to uncover the underlying molecular mechanisms of observed cross talk between CK action and ethylene biosynthesis in the regulation of RAM size.

In contrast to CKs, ethylene has been demonstrated to inhibit cell elongation in the root (Růžička et al., 2007). However, similar to the aforementioned CK-mediated regulation of RAM size, this was observed during long-term cultivation of Arabidopsis seedlings in the presence of excessive amounts of exogenous ACC. Under the conditions of our assay, we were unable to detect any BAP effects on cell elongation in the wild type and the *acs9* line, whereas *aco2* and particularly *atms1* exhibited large reductions in cell length. These results suggest that ethylene may interfere with immediate CK effects on root growth even at the level of cell elongation. The increased length of cells in mock-treated *atms1* is consistent with the negative role of ethylene in root elongation and suggests that a physiologically effective amount of ethylene was still present in the root. This is in agreement with our analysis of the ethylene-responsive reporter line (EBS:GUS), revealing GUS activity even in the mock-treated root (Supplemental Fig. S7). Consistently, the presence of 2-aminoethoxyvinylglycine, an inhibitor of ethylene biosynthesis, has also been shown to increase root cell length (Růžička et al., 2007).

In summary, our findings suggest that CKs and ethylene are tightly interconnected in their regulatory roles on root growth and imply that endogenous ethylene homeostasis is important for the CK-mediated regulation of individual RAM parameters (Fig. 7).

MATERIALS AND METHODS

Plant Material

The following lines of Arabidopsis (*Arabidopsis thaliana*) were used: *atms1* (Nottingham Arabidopsis Stock Centre; N833778), *acs9-1* (N676907), and *aco2* (N674747). Arabidopsis ecotype Columbia (Col-0; N1092) was used as a control. The EBS:GUS line was constructed by Anna Stepanova in the Joe Ecker laboratory.

Plant Growth Conditions

For proteome analysis, quantitative real-time PCR, and hormone measurements (CK, ABA, and ACC levels), seedlings were cultivated on square plates with nylon mesh (Uhelon 120T; Silk & Progress) positioned vertically in growth chambers (Percival Scientific; CLF Plant Climatics) under a 16/8-h light/dark photoperiod at 150 μmol m^{-2} s^{-1} as described previously (Pernisová et al., 2009). Six-day-old seedlings were treated with liquid MS medium containing 5 μM BAP (Duchefa) for 30 min or 2 h. For mock-treated samples, we used liquid MS medium supplemented with 0.1% dimethyl sulfoxide (DMSO). The treatment was carried out under gentle stirring in the growth chambers (Percival Scientific) under the same conditions as seedling cultivation. After the treatment, roots and shoots were detached with a scalpel, collected, immediately frozen in liquid nitrogen, and analyzed separately. For the proteome analysis, four independent biological replicates were performed, whereas for the quantitative real-time PCR and hormone measurements, three independent biological replicates were used.

In the root elongation assay and GUS staining assay, 6-d-old seedlings grown on vertical petri dishes and 1× MS medium were replanted into 1× MS medium supplemented with 100 nM BAP (Duchefa; dissolved in DMSO) and 0.01% DMSO as a control. After 2 d of incubation, root elongation was measured (ImageJ; National Institutes of Health; http://rsb.info.nih.gov/ij) and compared with the wild type (Col-0). At least 20 seedlings were evaluated in at least three independent experiments. An Olympus BX61 microscope using differential interference contrast microscopy was used for measurements of RAM lengths and root cell lengths. Root cell lengths were measured in the first fully elongated cortex cells following the transient zone. GUS staining was performed as described previously (Hejátko et al., 2003).

Proteomic Analysis

For two-dimensional gel electrophoresis, proteins were isolated separately from approximately 0.5 g fresh weight of the shoots and roots using the 10% TCA/acetate extraction method (Tsugita and Kamo, 1999). For isoelectric focusing (IEF; the first dimension of two-dimensional electrophoresis), vacuum-dried protein isolates were dissolved in IPG buffer (7 M urea, 2 M thiourea, 2% [w/v] CHAPS, 60 mM dithiothreitol [DTT], 0.8% Biolyte 3/10 Ampholyte [Bio-Rad], and 0.003% bromphenol blue) and the protein concentration was determined using a RC/DC kit (Bio-Rad). Solubilized protein samples were subjected to centrifugation at 20,000 relative centrifugal force for 60 min at 10°C before application onto IPG strips. A total of 150 μg

of whole protein sample in 315 μL of IPG buffer per IPG strip was applied to 18-cm ReadyStrip IPG strips, pH 3 to 10 nonlinear (Bio-Rad), by passive rehydration. IEF was performed in a Protean IEF Cell (Bio-Rad) for 80,000 Vh. Prior to the second dimension, the IPG strips were equilibrated in buffer (6 M urea, 0.375 M Tris-HCl, pH 8.8, 2% SDS, 20% glycerol, and 2% DTT) for 10 min, followed by 10 min in a second equilibration buffer containing 2.5% iodoacetamide instead of DTT.

For SDS-PAGE (the second dimension of two-dimensional electrophoresis), 12% vertical polyacrylamide gels were employed in a Protean Plus Dodeca Cell (Bio-Rad). The Precision Plus Protein Standard (Bio-Rad) was applied to each gel. Gels were stained with Sypro Ruby (Invitrogen) fluorescent dye according to the manufacturer's recommendations. Gels were scanned by FLA-7000 Fluorescent Image Analyzer (Fuji Film).

Image analysis of protein maps was performed using PDQuest 8.0.1 Advanced software (Bio-Rad). The Spot Detection Wizard was used to select the parameters for spot detection; a faint spot (the sensitivity and minimum peak value parameter) and a large spot cluster (the radius of the background subtraction) were selected. Gel warping was carried out prior to spot matching. The results of automated spot detection and matching were checked and, if necessary, manually corrected. On average, 1,900 protein spots were monitored on gels of shoot isolates, whereas around 1,500 protein spots were detected on gels of root isolates. Protein spots with an intensity at least 10-fold higher than the gel background on at least three out of four gel replicates were considered for further evaluation. A local regression model (Loess) was used for spot intensity normalization. For quantitative differentiation, a 1.5-fold change or higher in the average spot intensity between compared samples was regarded as significant. Statistical significance of differences was assessed using Student's *t* test at a significance level of 0.05 in four biological replicates. Individual protein spots selected on the basis of image-analysis output as those showing significant changes were excised using a spot cutter (Bio-Rad), in-gel digested with trypsin, and identified by liquid chromatography-tandem mass spectrometry (for details, see Supplemental Materials and Methods S1). All identified proteins in qualitatively different spots were considered (Supplemental Table S1A). Only spots with a single identified protein were considered for quantitative evaluation (Supplemental Table S1B).

Hormonal Analysis

For endogenous CK analysis, extraction and purification of approximately 0.2 g fresh weight was performed according to the method described previously, and levels of CKs were quantified by ultra-performance liquid chromatography-electrospray tandem mass spectrometry. For ABA and ACC measurements, samples were purified by solid-phase extraction and then derivatized and analyzed by gas chromatography-tandem mass spectrometry. For details see Supplemental Materials and Methods S1.

Supplemental Data

The following materials are available in the online version of this article.

Supplemental Figure S1. Mapping of BAP-regulated proteins in the processes dominantly affected in the shoot.

Supplemental Figure S2. Mapping of BAP-regulated proteins in the processes dominantly affected in the root.

Supplemental Figure S3. BAP regulates proteins involved in phytohormone biosynthesis.

Supplemental Figure S4. Exogenous BAP application modulates levels of endogenous CKs and their metabolites.

Supplemental Figure S5. Typical two-dimensional electrophoresis maps showing the quality of gel separation.

Supplemental Figure S6. RAM lengths and root cell lengths of mutants in ethylene biosynthesis in response to BAP.

Supplemental Figure S7. BAP-mediated ethylene production in ethylene-responsive reporter line EBS:GUS in the shoot (A) and root (B).

Supplemental Table S1. BAP-regulated proteins in Arabidopsis seedlings.

Supplemental Table S2. Overview of mapping BAP-regulated proteins in the KEGG database.

Supplemental Table S3. ABA-related proteins identified as BAP regulated in the shoot and root.

Supplemental Table S4. Overlay of proteins identified in our study with the ethylene-mediated proteome response in the whole seedling as identified by Chen et al. (2011).

Supplemental Materials and Methods S1.

Supplemental References S1.

ACKNOWLEDGMENTS

We thank E. Benkova, K. Růžička, and E. Meyerowitz for kindly reading the manuscript and providing valuable comments. We are grateful to Hillel Fromm for providing us with polyclonal antibody directed against the Arabidopsis recombinant prohibitin and Anna Stepanova, Joe Ecker, and Jose Alonso for the EBS:GUS line.

Received June 29, 2012; accepted November 30, 2012; published December 3, 2012.

LITERATURE CITED

Argueso CT, Ferreira FJ, Epple P, To JP, Hutchison CE, Schaller GE, Dangl JL, Kieber JJ (2012) Two-component elements mediate interactions between cytokinin and salicylic acid in plant immunity. PLoS Genet **8:** e1002448

Azimzadeh J, Nacry P, Christodoulidou A, Drevensek S, Camilleri C, Amiour N, Parcy F, Pastuglia M, Bouchez D (2008) *Arabidopsis* TONNEAU1 proteins are essential for preprophase band formation and interact with centrin. Plant Cell **20:** 2146–2159

Barroso C, Romero LC, Cejudo FJ, Vega JM, Gotor C (1999) Salt-specific regulation of the cytosolic O-acetylserine(thiol)lyase gene from Arabidopsis thaliana is dependent on abscisic acid. Plant Mol Biol **40:** 729–736

Bédard J, Kubis S, Bimanadham S, Jarvis P (2007) Functional similarity between the chloroplast translocon component, Tic40, and the human co-chaperone, Hsp70-interacting protein (Hip). J Biol Chem **282:** 21404–21414

Bevan M, Bancroft I, Bent E, Love K, Goodman H, Dean C, Bergkamp R, Dirkse W, Van Staveren M, Stiekema W, et al (1998) Analysis of 1.9 Mb of contiguous sequence from chromosome 4 of Arabidopsis thaliana. Nature **391:** 485–488

Brenner WG, Ramireddy E, Heyl A, Schmulling T (2012) Gene regulation by cytokinin in Arabidopsis. Front Plant Sci **3:** 8

Brenner WG, Romanov GA, Köllmer I, Bürkle L, Schmülling T (2005) Immediate-early and delayed cytokinin response genes of Arabidopsis thaliana identified by genome-wide expression profiling reveal novel cytokinin-sensitive processes and suggest cytokinin action through transcriptional cascades. Plant J **44:** 314–333

Brenner WG, Schmulling T (2012) Transcript profiling of cytokinin action in Arabidopsis roots and shoots discovers largely similar but also organ-specific responses. BMC Plant Biol **12:** 112

Caesar K, Thamm AM, Witthöft J, Elgass K, Huppenberger P, Grefen C, Horak J, Harter K (2011) Evidence for the localization of the Arabidopsis cytokinin receptors AHK3 and AHK4 in the endoplasmic reticulum. J Exp Bot **62:** 5571–5580

Cary AJ, Liu W, Howell SH (1995) Cytokinin action is coupled to ethylene in its effects on the inhibition of root and hypocotyl elongation in *Arabidopsis thaliana* seedlings. Plant Physiol **107:** 1075–1082

Černý M, Dyčka F, Bobál'ová J, Brzobohatý B (2011) Early cytokinin response proteins and phosphoproteins of Arabidopsis thaliana identified by proteome and phosphoproteome profiling. J Exp Bot **62:** 921–937

Chae HS, Faure F, Kieber JJ (2003) The *eto1*, *eto2*, and *eto3* mutations and cytokinin treatment increase ethylene biosynthesis in *Arabidopsis* by increasing the stability of ACS protein. Plant Cell **15:** 545–559

Chen R, Binder BM, Garrett WM, Tucker ML, Chang C, Cooper B (2011) Proteomic responses in Arabidopsis thaliana seedlings treated with ethylene. Mol Biosyst **7:** 2637–2650

Choi J, Huh SU, Kojima M, Sakakibara H, Paek KH, Hwang I (2010) The cytokinin-activated transcription factor ARR2 promotes plant immunity via TGA3/NPR1-dependent salicylic acid signaling in Arabidopsis. Dev Cell **19:** 284–295

Dello Ioio R, Linhares FS, Scacchi E, Casamitjana-Martinez E, Heidstra R, Costantino P, Sabatini S (2007) Cytokinins determine Arabidopsis root-meristem size by controlling cell differentiation. Curr Biol **17:** 678–682

Desveaux D, Subramaniam R, Després C, Mess JN, Lévesque C, Fobert PR, Dangl JL, Brisson N (2004) A "Whirly" transcription factor is required for salicylic acid-dependent disease resistance in Arabidopsis. Dev Cell **6:** 229–240

Dinneny JR, Benfey PN (2008) Plant stem cell niches: standing the test of time. Cell **132:** 553–557

Foss EJ, Radulovic D, Shaffer SA, Ruderfer DM, Bedalov A, Goodlett DR, Kruglyak L (2007) Genetic basis of proteome variation in yeast. Nat Genet **39:** 1369–1375

Fu H, Girod PA, Doelling JH, van Nocker S, Hochstrasser M, Finley D, Vierstra RD (1999) Structure and functional analysis of the 26S proteasome subunits from plants. Mol Biol Rep **26:** 137–146

Fu J, Keurentjes JJ, Bouwmeester H, America T, Verstappen FW, Ward JL, Beale MH, de Vos RC, Dijkstra M, Scheltema RA, et al (2009) System-wide molecular evidence for phenotypic buffering in Arabidopsis. Nat Genet **41:** 166–167

Gajdošová S, Spíchal L, Kamínek M, Hoyerová K, Novák O, Dobrev PI, Galuszka P, Klíma P, Gaudinová A, Žižková E, et al (2011) Distribution, biological activities, metabolism, and the conceivable function of cis-zeatin-type cytokinins in plants. J Exp Bot **62:** 2827–2840

Ghazalpour A, Bennett B, Petyuk VA, Orozco L, Hagopian R, Mungrue IN, Farber CR, Sinsheimer J, Kang HM, Furlotte N, et al (2011) Comparative analysis of proteome and transcriptome variation in mouse. PLoS Genet **7:** e1001393

Ghelis T, Bolbach G, Clodic G, Habricot Y, Miginiac E, Sotta B, Jeannette E (2008) Protein tyrosine kinases and protein tyrosine phosphatases are involved in abscisic acid-dependent processes in Arabidopsis seeds and suspension cells. Plant Physiol **148:** 1668–1680

Hansen M, Chae HS, Kieber JJ (2009) Regulation of ACS protein stability by cytokinin and brassinosteroid. Plant J **57:** 606–614

Hejátko J, Pernisová M, Eneva T, Palme K, Brzobohatý B (2003) The putative sensor histidine kinase CKI1 is involved in female gametophyte development in Arabidopsis. Mol Genet Genomics **269:** 443–453

Hwang I, Sheen J, Müller B (2012) Cytokinin signaling networks. Annu Rev Plant Biol **63:** 353–380

Ishiguro S, Watanabe Y, Ito N, Nonaka H, Takeda N, Sakai T, Kanaya H, Okada K (2002) SHEPHERD is the Arabidopsis GRP94 responsible for the formation of functional CLAVATA proteins. EMBO J **21:** 898–908

Kasahara H, Hanada A, Kuzuyama T, Takagi M, Kamiya Y, Yamaguchi S (2002) Contribution of the mevalonate and methylerythritol phosphate pathways to the biosynthesis of gibberellins in Arabidopsis. J Biol Chem **277:** 45188–45194

Kasahara H, Takei K, Ueda N, Hishiyama S, Yamaya T, Kamiya Y, Yamaguchi S, Sakakibara H (2004) Distinct isoprenoid origins of cis- and trans-zeatin biosyntheses in Arabidopsis. J Biol Chem **279:** 14049–14054

Kim K, Ryu H, Cho YH, Scacchi E, Sabatini S, Hwang I (2012) Cytokinin-facilitated proteolysis of ARABIDOPSIS RESPONSE REGULATOR 2 attenuates signaling output in two-component circuitry. Plant J **69:** 934–945

Kurakawa T, Ueda N, Maekawa M, Kobayashi K, Kojima M, Nagato Y, Sakakibara H, Kyozuka J (2007) Direct control of shoot meristem activity by a cytokinin-activating enzyme. Nature **445:** 652–655

Kyozuka J (2007) Control of shoot and root meristem function by cytokinin. Curr Opin Plant Biol **10:** 442–446

Marhavý P, Bielach A, Abas L, Abuzeineh A, Duclercq J, Tanaka H, Pařezová M, Petrášek J, Friml J, Kleine-Vehn J, et al (2011) Cytokinin modulates endocytic trafficking of PIN1 auxin efflux carrier to control plant organogenesis. Dev Cell **21:** 796–804

Milborrow BV (2001) The pathway of biosynthesis of abscisic acid in vascular plants: a review of the present state of knowledge of ABA biosynthesis. J Exp Bot **52:** 1145–1164

Mok MC (1994) Cytokinins and plant development: an overview. *In* DWS Mok, MC Mok, eds, Cytokinins: Chemistry, Activity, and Function. CRC Press, Boca Raton, FL, pp 155–166

Ning K, Fermin D, Nesvizhskii AI (2012) Comparative analysis of different label-free mass spectrometry based protein abundance estimates and their correlation with RNA-Seq gene expression data. J Proteome Res **11:** 2261–2271

Nishiyama R, Watanabe Y, Fujita Y, Le DT, Kojima M, Werner T, Vankova R, Yamaguchi-Shinozaki K, Shinozaki K, Kakimoto T, et al (2011) Analysis of cytokinin mutants and regulation of cytokinin metabolic genes reveals important regulatory roles of cytokinins in drought, salt and abscisic acid responses, and abscisic acid biosynthesis. Plant Cell **23:** 2169–2183

Pernisová M, Klíma P, Horák J, Válková M, Malbeck J, Souček P, Reichman P, Hoyerová K, Dubová J, Friml J, et al (2009) Cytokinins modulate auxin-induced organogenesis in plants via regulation of the auxin efflux. Proc Natl Acad Sci USA **106:** 3609–3614

Rashotte AM, Carson SD, To JP, Kieber JJ (2003) Expression profiling of cytokinin action in Arabidopsis. Plant Physiol **132:** 1998–2011

Reski R (1994) Plastid genes and chloroplast biogenesis. *In* DWS Mok, MC Mok, eds, Cytokinins: Chemistry, Activity, and Function. CRC Press, Boca Raton, FL, pp 179–195

Růžička K, Ljung K, Vanneste S, Podhorská R, Beeckman T, Friml J, Benková E (2007) Ethylene regulates root growth through effects on auxin biosynthesis and transport-dependent auxin distribution. Plant Cell **19:** 2197–2212

Růžička K, Simásková M, Duclercq J, Petrášek J, Zažímalová E, Simon S, Friml J, Van Montagu MC, Benková E (2009) Cytokinin regulates root meristem activity via modulation of the polar auxin transport. Proc Natl Acad Sci USA **106:** 4284–4289

Ryu MY, Cho SK, Kim WT (2009) RNAi suppression of RPN12a decreases the expression of type-A ARRs, negative regulators of cytokinin signaling pathway, in Arabidopsis. Mol Cells **28:** 375–382

Sakakibara H (2010) Cytokinin biosynthesis and metabolism. *In* PJ Davies, ed, Plant Hormones: Biosynthesis, Signal Transduction, Action! Ed 3. Springer, Dordrecht, The Netherlands, pp 95–114

Sakakibara H, Takei K, Hirose N (2006) Interactions between nitrogen and cytokinin in the regulation of metabolism and development. Trends Plant Sci **11:** 440–448

Saleem M, Lamkemeyer T, Schützenmeister A, Madlung J, Sakai H, Piepho HP, Nordheim A, Hochholdinger F (2010) Specification of cortical parenchyma and stele of maize primary roots by asymmetric levels of auxin, cytokinin, and cytokinin-regulated proteins. Plant Physiol **152:** 4–18

Smalle J, Kurepa J, Yang P, Babiychuk E, Kushnir S, Durski A, Vierstra RD (2002) Cytokinin growth responses in Arabidopsis involve the 26S proteasome subunit RPN12. Plant Cell **14:** 17–32

Solano R, Stepanova A, Chao Q, Ecker JR (1998) Nuclear events in ethylene signaling: a transcriptional cascade mediated by ETHYLENE-INSENSITIVE3 and ETHYLENE-RESPONSE-FACTOR1. Genes Dev **12:** 3703–3714

Spíchal L, Rakova NY, Riefler M, Mizuno T, Romanov GA, Strnad M, Schmülling T (2004) Two cytokinin receptors of Arabidopsis thaliana, CRE1/AHK4 and AHK3, differ in their ligand specificity in a bacterial assay. Plant Cell Physiol **45:** 1299–1305

Stahl Y, Simon R (2010) Plant primary meristems: shared functions and regulatory mechanisms. Curr Opin Plant Biol **13:** 53–58

Tanaka Y, Sano T, Tamaoki M, Nakajima N, Kondo N, Hasezawa S (2006) Cytokinin and auxin inhibit abscisic acid-induced stomatal closure by enhancing ethylene production in Arabidopsis. J Exp Bot **57:** 2259–2266

Taniguchi Y, Choi PJ, Li GW, Chen H, Babu M, Hearn J, Emili A, Xie XS (2010) Quantifying E. coli proteome and transcriptome with single-molecule sensitivity in single cells. Science **329:** 533–538

Tsugita A, Kamo M (1999) 2-D electrophoresis of plant proteins. Methods Mol Biol **112:** 95–97

Veach YK, Martin RC, Mok DW, Malbeck J, Vaňková R, Mok MC (2003) *O*-Glucosylation of cis-zeatin in maize: characterization of genes, enzymes, and endogenous cytokinins. Plant Physiol **131:** 1374–1380

Wareing PF, Khalifa MM, Treharne KJ (1968) Rate-limiting processes in photosynthesis at saturating light intensities. Nature **220:** 453–457

Watanabe N, Yokota T, Takahashi N (1982) Transfer-RNA, a possible supplier of free cytokinins, ribosyl-cis-zeatin and ribosyl-2-methylthiozeatin: quantitative comparison between free and transfer cytokinins in various tissues of the hop plant. Plant Cell Physiol **23:** 479–488

Werner T, Holst K, Pörs Y, Guivarc'h A, Mustroph A, Chriqui D, Grimm B, Schmülling T (2008) Cytokinin deficiency causes distinct changes of

sink and source parameters in tobacco shoots and roots. J Exp Bot **59:** 2659–2672

Werner T, Motyka V, Laucou V, Smets R, Van Onckelen H, Schmülling T (2003) Cytokinin-deficient transgenic *Arabidopsis* plants show multiple developmental alterations indicating opposite functions of cytokinins in the regulation of shoot and root meristem activity. Plant Cell **15:** 2532–2550

Werner T, Schmülling T (2009) Cytokinin action in plant development. Curr Opin Plant Biol **12:** 527–538

Wulfetange K, Lomin SN, Romanov GA, Stolz A, Heyl A, Schmülling T (2011) The cytokinin receptors of Arabidopsis are located mainly to the endoplasmic reticulum. Plant Physiol **156:** 1808–1818

Yoo HH, Kwon C, Lee MM, Chung IK (2007) Single-stranded DNA binding factor AtWHY1 modulates telomere length homeostasis in Arabidopsis. Plant J **49:** 442–451

Zhang W, To JP, Cheng CY, Eric Schaller G, Kieber JJ (2011) Type-A response regulators are required for proper root apical meristem function through post-transcriptional regulation of PIN auxin efflux carriers. Plant J **68:** 1–10

Supplemental Figure 1. Mapping of BAP-regulated proteins in the processes dominantly affected in the shoot. (A) Overview of BAP-regulated proteins mapped into the carbohydrate and energy metabolic pathways. Stars indicate proteins that were found in mixed spots on the 2-D gels; the background map was modified from the *Arabidopsis thaliana* 'Metabolic pathways' map in KEGG (Ogata et al., 1999). (B) BAP-regulated proteins mapped into the glycolysis/gluconeogenesis, (C) pyruvate metabolism, (D) carbon fixation processes, (E) citrate cycle and (F) ascorbate metabolism. In A-F, proteins regulated in the shoot are framed within continuous lines, whereas those regulated in the root are framed within dashed lines. **Down-regulated** proteins are indicated in red and **up-regulated** ones in green. Proteins that are upregulated or downregulated after 120 minutes (delayed response) are underlined. Proteins were mapped using the *Arabidopsis thaliana* KEGG Pathway tool (Ogata et al., 1999).

A

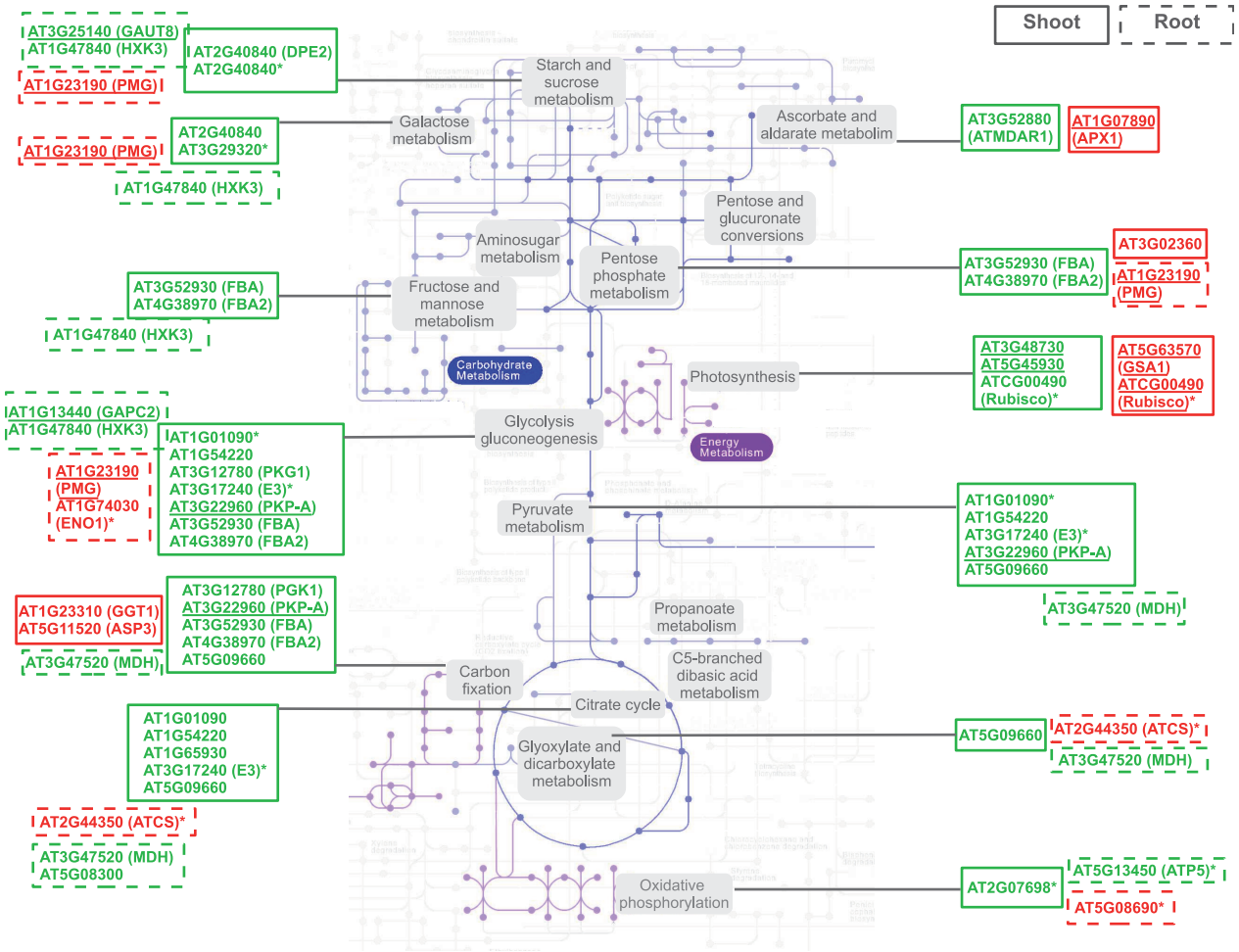

B

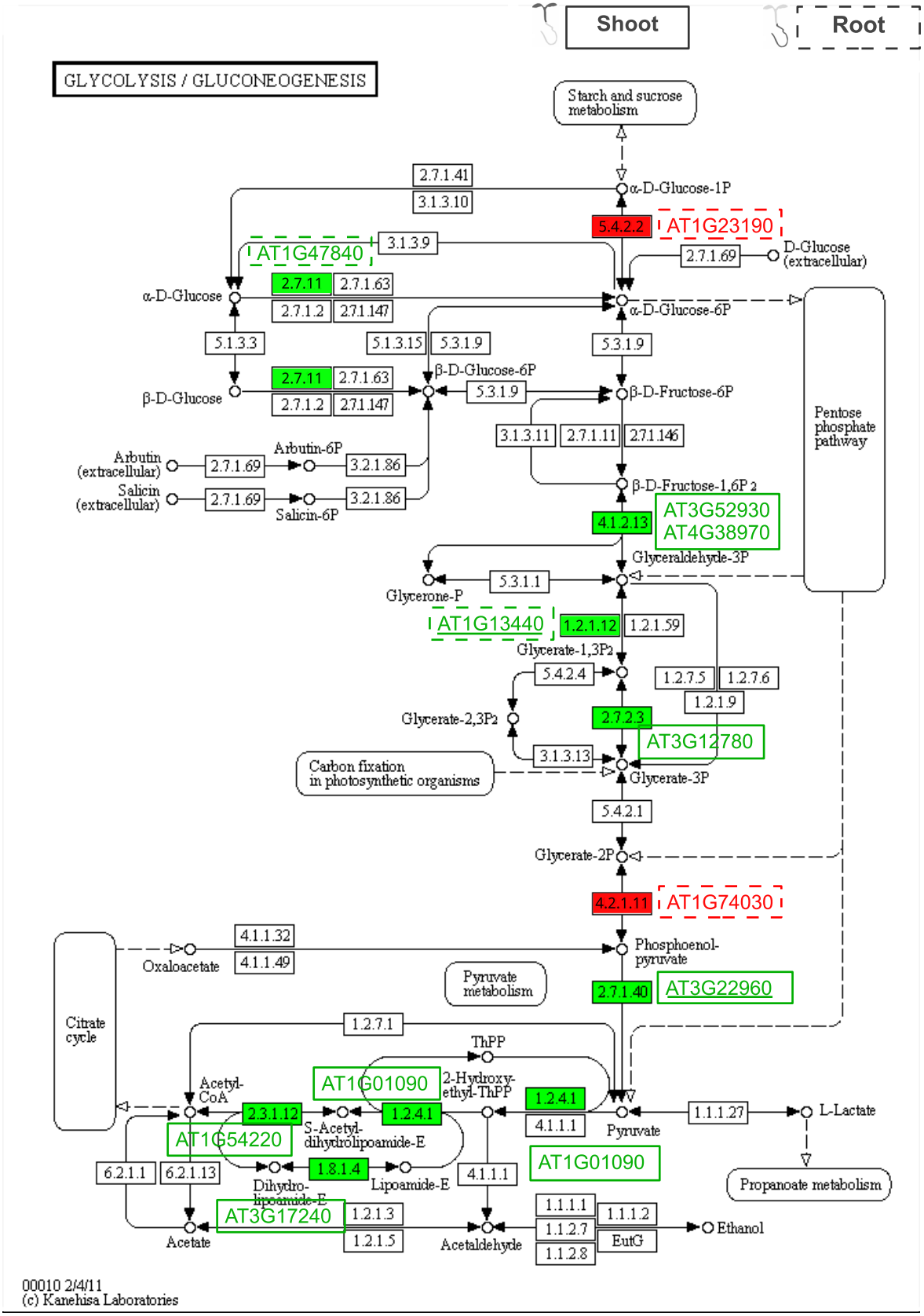
Shoot
Root
GLYCOLYSIS / GLUCONEOGENESIS
Starch and sucrose metabolism
α-D-Glucose-1P
2.7.1.41
3.1.3.10
5.4.2.2
AT1G23190
AT1G47840
3.1.3.9
2.7.1.69
D-Glucose (extracellular)
α-D-Glucose
2.7.11
2.7.1.63
2.7.1.2
2.7.1.147
α-D-Glucose-6P
5.1.3.3
5.1.3.15
5.3.1.9
β-D-Glucose-6P
β-D-Glucose
β-D-Fructose-6P
Pentose phosphate pathway
Arbutin (extracellular)
Arbutin-6P
Salicin (extracellular)
Salicin-6P
3.2.1.86
3.1.3.11
2.7.1.11
2.7.1.146
β-D-Fructose-1,6P 2
4.1.2.13
AT3G52930
AT4G38970
Glyceraldehyde-3P
Glycerone-P
AT1G13440
1.2.1.12
1.2.1.59
Glycerate-1,3P2
5.4.2.4
1.2.7.5
1.2.7.6
1.2.1.9
Glycerate-2,3P2
2.7.2.3
AT3G12780
3.1.3.13
Carbon fixation in photosynthetic organisms
Glycerate-3P
5.4.2.1
Glycerate-2P
4.2.1.11
AT1G74030
4.1.1.32
4.1.1.49
Oxaloacetate
Phosphoenol-pyruvate
Pyruvate metabolism
2.7.1.40
AT3G22960
Citrate cycle
1.2.7.1
ThPP
AT1G01090
2-Hydroxy-ethyl-ThPP
Acetyl-CoA
2.3.1.12
1.2.4.1
1.2.4.1
4.1.1.1
Pyruvate
1.1.1.27
L-Lactate
AT1G54220
S-Acetyl-dihydrolipoamide-E
AT1G01090
6.2.1.1
6.2.1.13
1.8.1.4
Dihydro-lipoamide-E
Lipoamide-E
4.1.1.1
Propanoate metabolism
AT3G17240
1.2.1.3
1.2.1.5
Acetate
Acetaldehyde
1.1.1.1
1.1.2.7
1.1.2.8
1.1.1.2
EutG
Ethanol
00010 2/4/11
(c) Kanehisa Laboratories

C

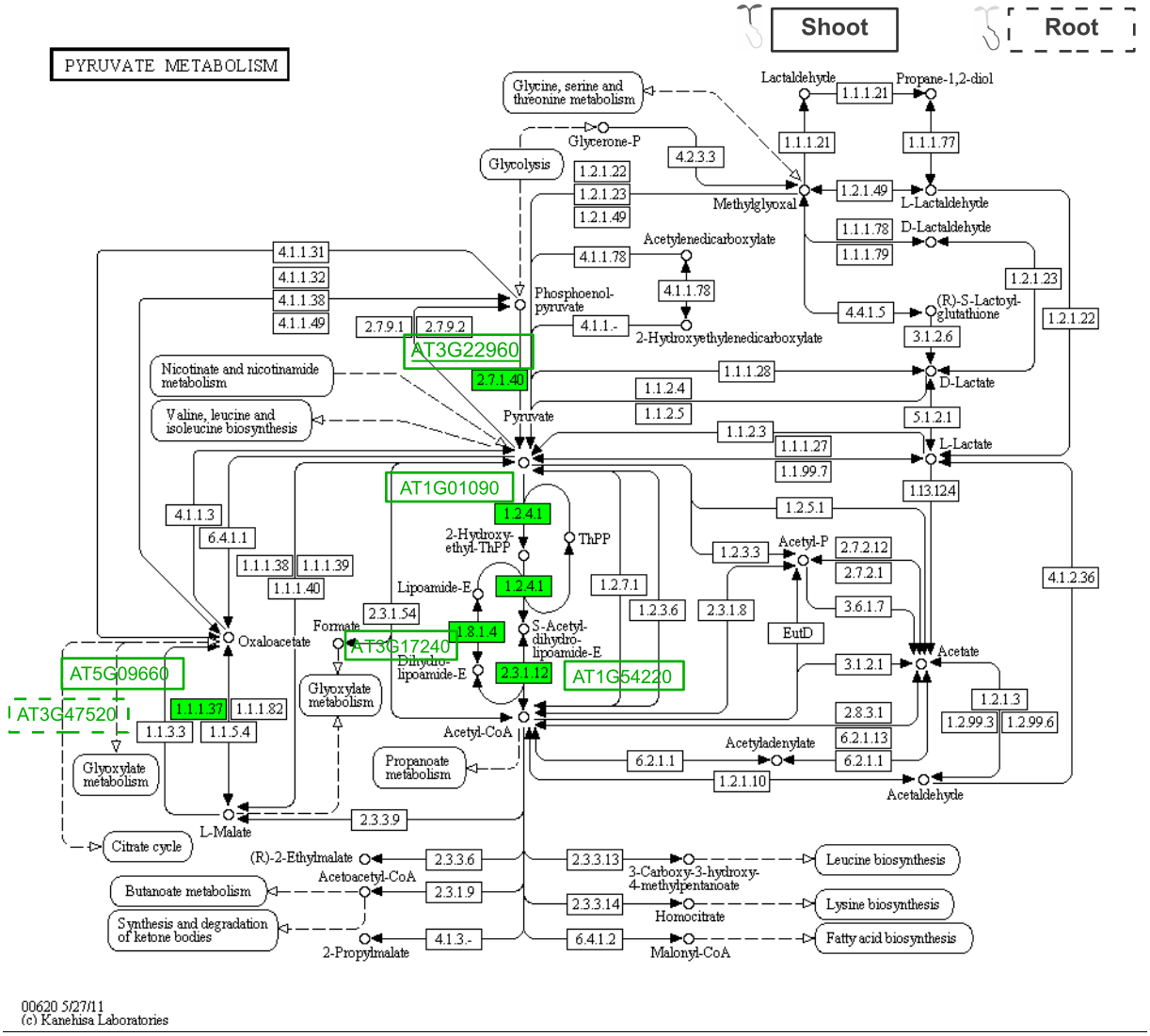
Shoot
Root
PYRUVATE METABOLISM
Glycine, serine and threonine metabolism
Glycerone-P
Glycolysis
Lactaldehyde
Propane-1,2-diol
Methylglyoxal
L-Lactaldehyde
D-Lactaldehyde
Acetylenedicarboxylate
Phosphoenol-pyruvate
2-Hydroxyethylenedicarboxylate
(R)-S-Lactoyl-glutathione
AT3G22960
Nicotinate and nicotinamide metabolism
Valine, leucine and isoleucine biosynthesis
Pyruvate
D-Lactate
L-Lactate
AT1G01090
2-Hydroxy-ethyl-ThPP
ThPP
Lipoamide-E
Dihydro-lipoamide-E
S-Acetyl-dihydro-lipoamide-E
Formate
AT3G17240
AT1G54220
Acetyl-P
Acetate
EutD
Oxaloacetate
AT5G09660
AT3G47520
Glyoxylate metabolism
Acetyl-CoA
Propanoate metabolism
Acetyladenylate
Acetaldehyde
L-Malate
Citrate cycle
(R)-2-Ethylmalate
Acetoacetyl-CoA
3-Carboxy-3-hydroxy-4-methylpentanoate
Leucine biosynthesis
Butanoate metabolism
Homocitrate
Lysine biosynthesis
Synthesis and degradation of ketone bodies
2-Propylmalate
Malonyl-CoA
Fatty acid biosynthesis
00620 5/27/11
(c) Kanehisa Laboratories

D

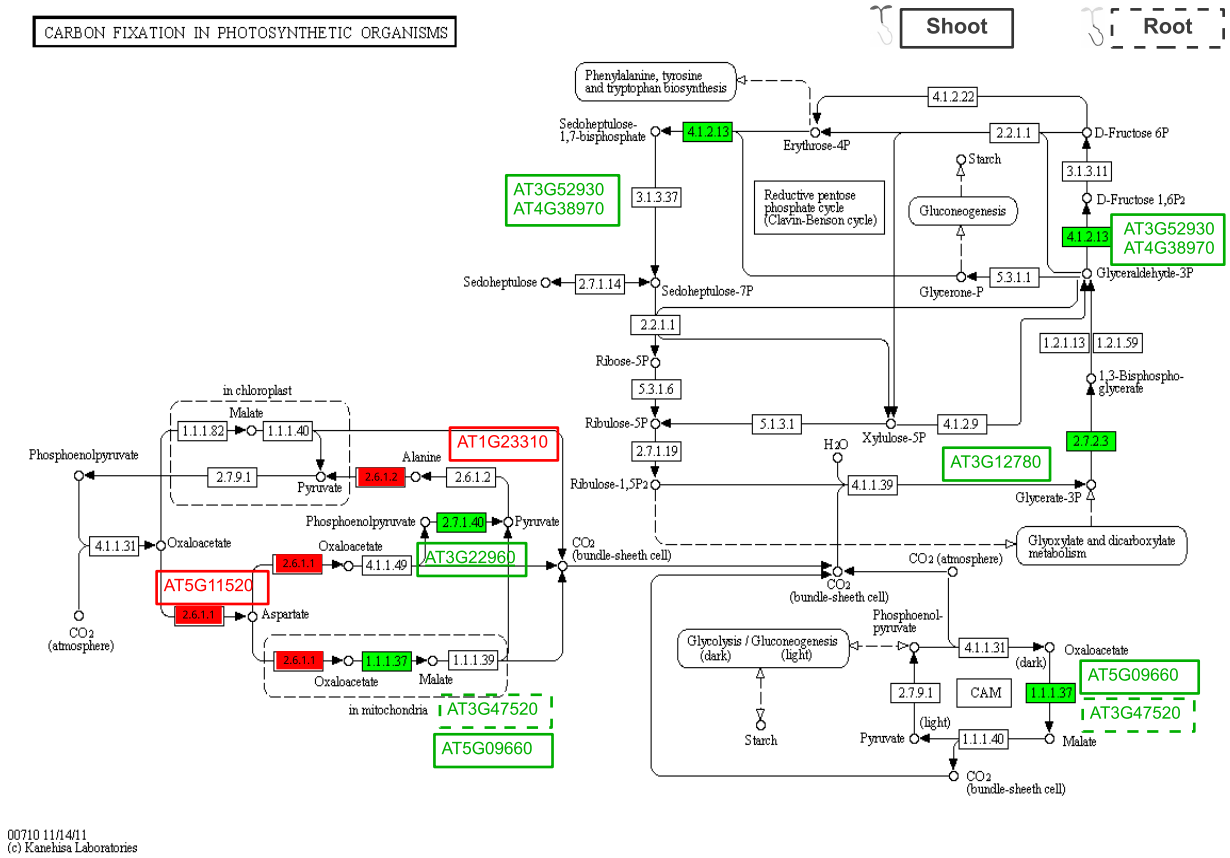
CARBON FIXATION IN PHOTOSYNTHETIC ORGANISMS
Shoot
Root
Phenylalanine, tyrosine and tryptophan biosynthesis
4.1.2.22
Sedoheptulose-1,7-bisphosphate
4.1.2.13
Erythrose-4P
2.2.1.1
D-Fructose 6P
Starch
3.1.3.11
AT3G52930
AT4G38970
3.1.3.37
Reductive pentose phosphate cycle (Calvin-Benson cycle)
Gluconeogenesis
D-Fructose 1,6P2
4.1.2.13
AT3G52930
AT4G38970
Sedoheptulose
2.7.1.14
Sedoheptulose-7P
Glycerone-P
5.3.1.1
Glyceraldehyde-3P
2.2.1.1
1.2.1.13
1.2.1.59
Ribose-5P
1,3-Bisphospho-glycerate
5.3.1.6
in chloroplast
Malate
1.1.1.82
1.1.1.40
AT1G23310
Ribulose-5P
5.1.3.1
Xylulose-5P
4.1.2.9
2.7.2.3
Phosphoenolpyruvate
2.7.9.1
Pyruvate
Alanine
2.6.1.2
2.6.1.2
2.7.1.19
H2O
AT3G12780
Ribulose-1,5P2
4.1.1.39
Glycerate-3P
Phosphoenolpyruvate
2.7.1.40
Pyruvate
4.1.1.31
Oxaloacetate
Oxaloacetate
2.6.1.1
4.1.1.49
AT3G22960
CO2 (bundle-sheeth cell)
CO2 (atmosphere)
Glyoxylate and dicarboxylate metabolism
AT5G11520
CO2 (bundle-sheeth cell)
2.6.1.1
Aspartate
Phosphoenol-pyruvate
CO2 (atmosphere)
Glycolysis / Gluconeogenesis (dark) (light)
4.1.1.31
Oxaloacetate
(dark)
AT5G09660
2.6.1.1
1.1.1.37
1.1.1.39
2.7.9.1
CAM
1.1.1.37
AT3G47520
Oxaloacetate
Malate
in mitochondria
AT3G47520
(light)
Starch
Pyruvate
1.1.1.40
Malate
AT5G09660
CO2 (bundle-sheeth cell)
00710 11/14/11
(c) Kanehisa Laboratories

E

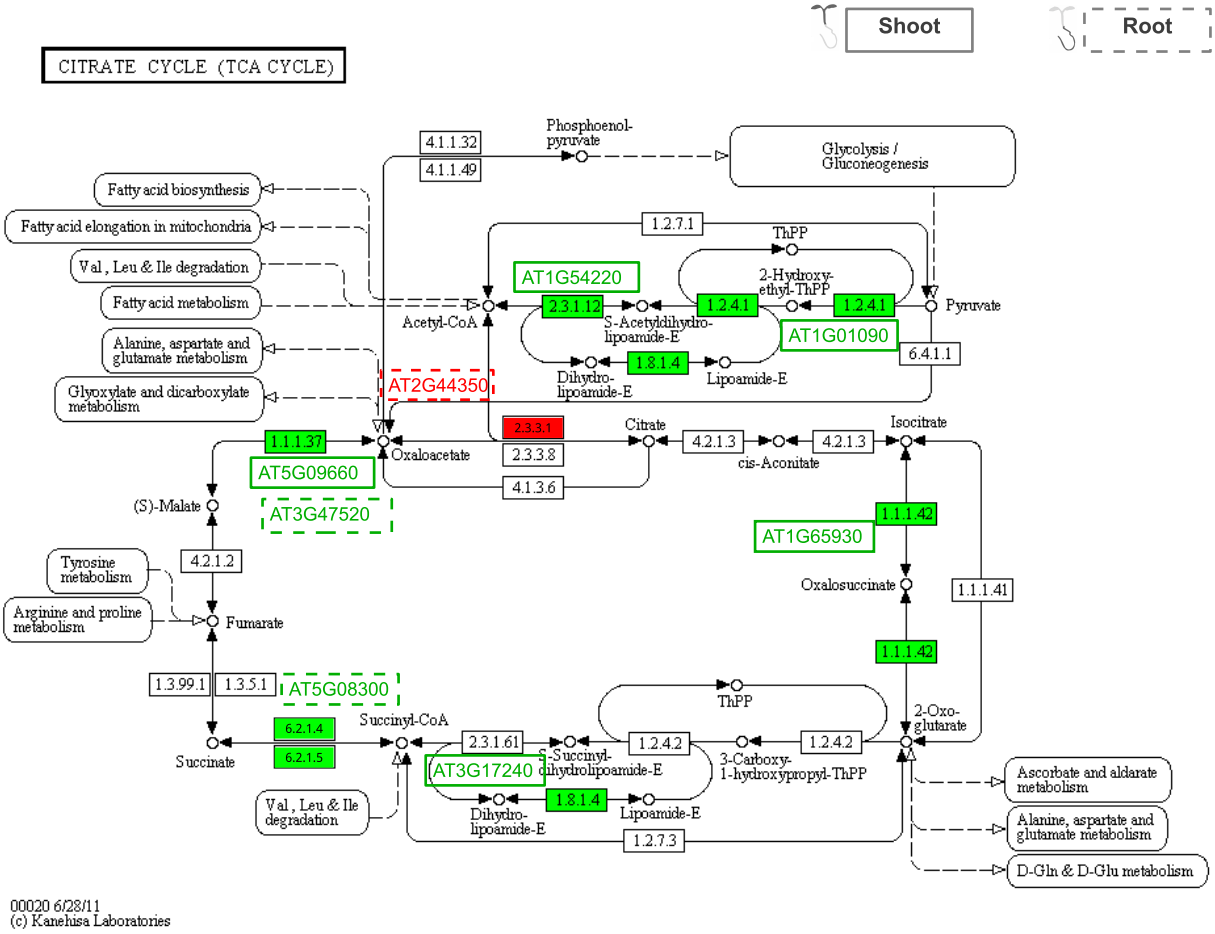
Shoot
Root
CITRATE CYCLE (TCA CYCLE)
Phosphoenol-pyruvate
4.1.1.32
4.1.1.49
Glycolysis / Gluconeogenesis
Fatty acid biosynthesis
Fatty acid elongation in mitochondria
Val , Leu & Ile degradation
Fatty acid metabolism
Alanine, aspartate and glutamate metabolism
Glyoxylate and dicarboxylate metabolism
1.2.7.1
ThPP
AT1G54220
2-Hydroxy-ethyl-ThPP
2.3.1.12
1.2.4.1
1.2.4.1
Pyruvate
Acetyl-CoA
S-Acetyldihydro-lipoamide-E
AT1G01090
6.4.1.1
1.8.1.4
Dihydro-lipoamide-E
Lipoamide-E
AT2G44350
2.3.3.1
Citrate
4.2.1.3
4.2.1.3
Isocitrate
1.1.1.37
Oxaloacetate
2.3.3.8
cis-Aconitate
AT5G09660
4.1.3.6
(S)-Malate
AT3G47520
1.1.1.42
AT1G65930
Tyrosine metabolism
4.2.1.2
Oxalosuccinate
1.1.1.41
Arginine and proline metabolism
Fumarate
1.1.1.42
1.3.99.1
1.3.5.1
AT5G08300
ThPP
2-Oxo-glutarate
6.2.1.4
Succinyl-CoA
2.3.1.61
1.2.4.2
1.2.4.2
6.2.1.5
AT3G17240
S-Succinyl-dihydrolipoamide-E
3-Carboxy-1-hydroxypropyl-ThPP
Succinate
Ascorbate and aldarate metabolism
1.8.1.4
Val , Leu & Ile degradation
Dihydro-lipoamide-E
Lipoamide-E
Alanine, aspartate and glutamate metabolism
1.2.7.3
D-Gln & D-Glu metabolism
00020 6/28/11
(c) Kanehisa Laboratories

F

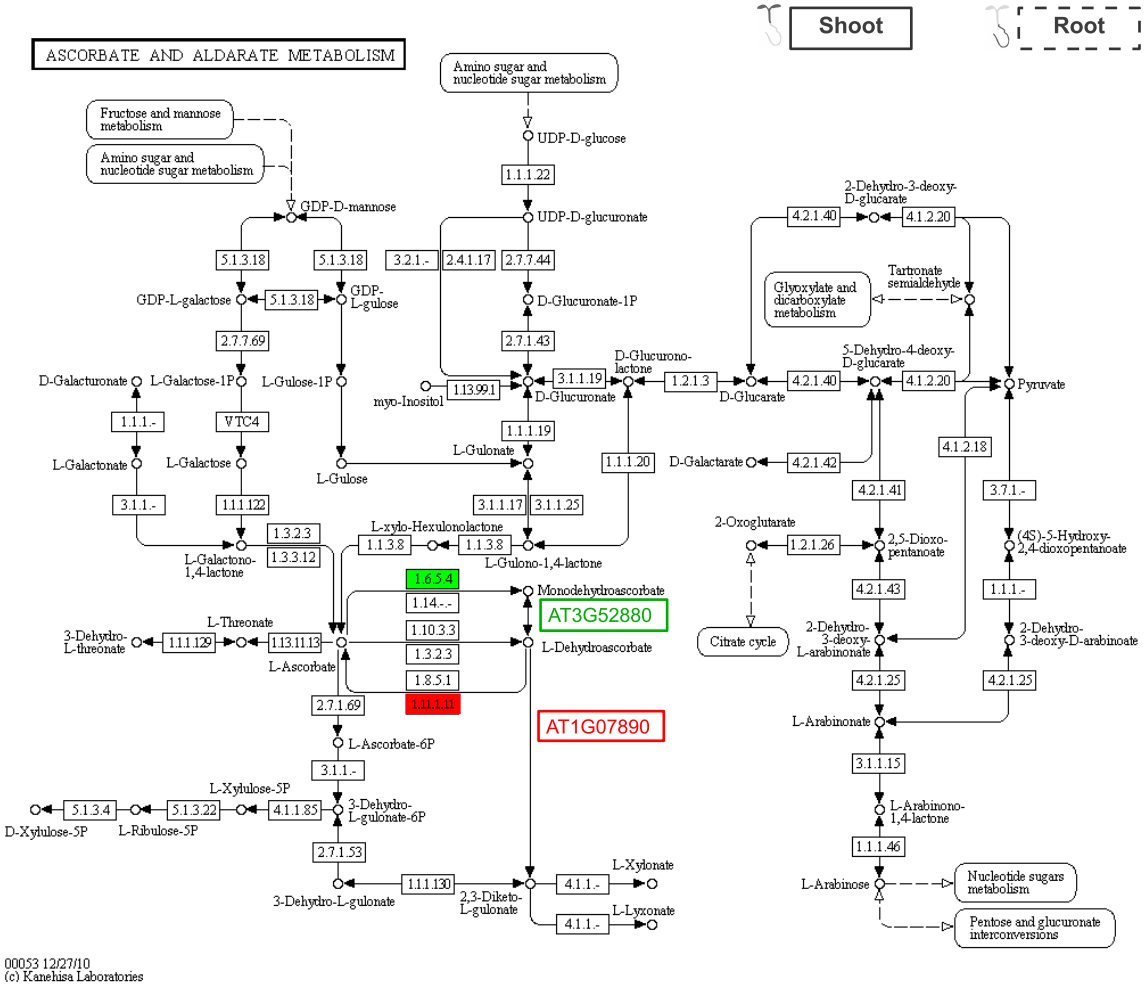
Shoot
Root
ASCORBATE AND ALDARATE METABOLISM
Amino sugar and nucleotide sugar metabolism
Fructose and mannose metabolism
Amino sugar and nucleotide sugar metabolism
UDP-D-glucose
1.1.1.22
GDP-D-mannose
UDP-D-glucuronate
5.1.3.18
5.1.3.18
3.2.1.-
2.4.1.17
2.7.7.44
GDP-L-galactose
5.1.3.18
GDP-L-gulose
D-Glucuronate-1P
2.7.7.69
2.7.1.43
D-Galacturonate
L-Galactose-1P
L-Gulose-1P
myo-Inositol
1.13.99.1
3.1.1.19
D-Glucuronate
D-Glucurono-lactone
1.2.1.3
D-Glucarate
4.2.1.40
4.1.2.20
Pyruvate
1.1.1.-
VTC4
1.1.1.19
L-Gulonate
L-Galactonate
L-Galactose
L-Gulose
1.1.1.20
D-Galactarate
4.2.1.42
4.1.2.18
3.1.1.-
1.1.1.122
3.1.1.17
3.1.1.25
4.2.1.41
3.7.1.-
1.3.2.3
L-xylo-Hexulonolactone
2-Oxoglutarate
1.2.1.26
2,5-Dioxo-pentanoate
(4S)-5-Hydroxy-2,4-dioxopentanoate
L-Galactono-1,4-lactone
1.3.3.12
1.1.3.8
1.1.3.8
L-Gulono-1,4-lactone
1.6.5.4
Monodehydroascorbate
4.2.1.43
1.1.1.-
1.14.-.-
AT3G52880
L-Threonate
1.10.3.3
3-Dehydro-L-threonate
1.1.1.129
1.13.11.13
1.3.2.3
L-Dehydroascorbate
Citrate cycle
2-Dehydro-3-deoxy-L-arabinonate
2-Dehydro-3-deoxy-D-arabinoate
L-Ascorbate
1.8.5.1
1.11.1.11
4.2.1.25
4.2.1.25
2.7.1.69
AT1G07890
L-Ascorbate-6P
L-Arabinonate
3.1.1.-
3.1.1.15
L-Xylulose-5P
5.1.3.4
5.1.3.22
4.1.1.85
3-Dehydro-L-gulonate-6P
L-Arabinono-1,4-lactone
D-Xylulose-5P
L-Ribulose-5P
1.1.1.46
2.7.1.53
L-Xylonate
L-Arabinose
Nucleotide sugars metabolism
1.1.1.130
4.1.1.-
3-Dehydro-L-gulonate
2,3-Diketo-L-gulonate
4.1.1.-
L-Lyxonate
Pentose and glucuronate interconversions
00053 12/27/10
(c) Kanehisa Laboratories

Supplemental Figure 2. Mapping of BAP-regulated proteins in the processes dominantly affected in the root. (A) Mapping of BAP-regulated proteins into the RNA transport, (B) protein degradation by proteasome, (C) ER processing, (D) amino sugar and nucleotide sugar metabolism and (E) cysteine and methionine metabolism. In A-E, proteins regulated in the shoot are framed within continuous lines, while those regulated in the root are framed within dashed lines. **Down-regulated** proteins are indicated in red and **up-regulated** ones in green. Proteins that are upregulated or downregulated after 120 minutes (delayed response) are underlined. Proteins were mapped using the *Arabidopsis thaliana* KEGG Pathway tool (Ogata et al., 1999).

A

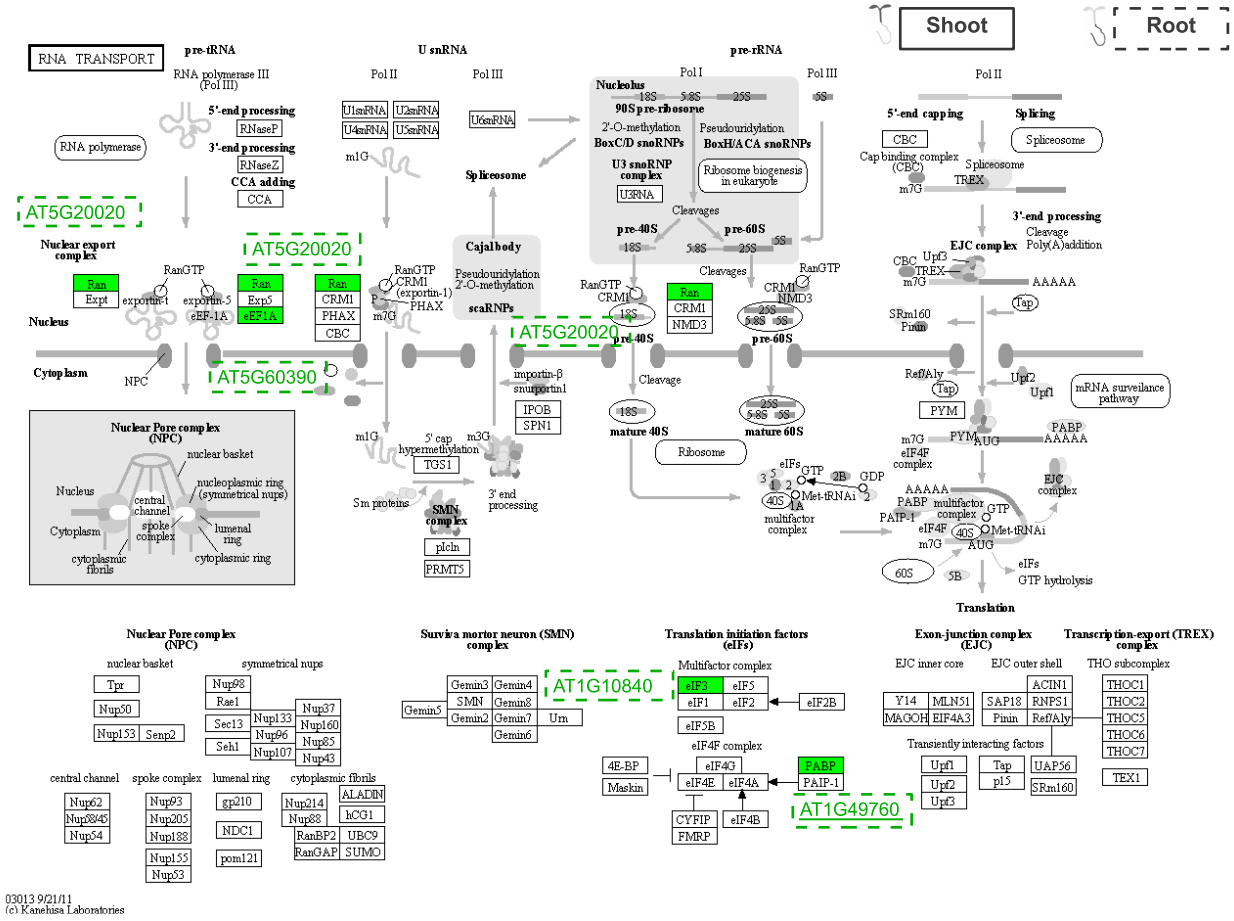

B

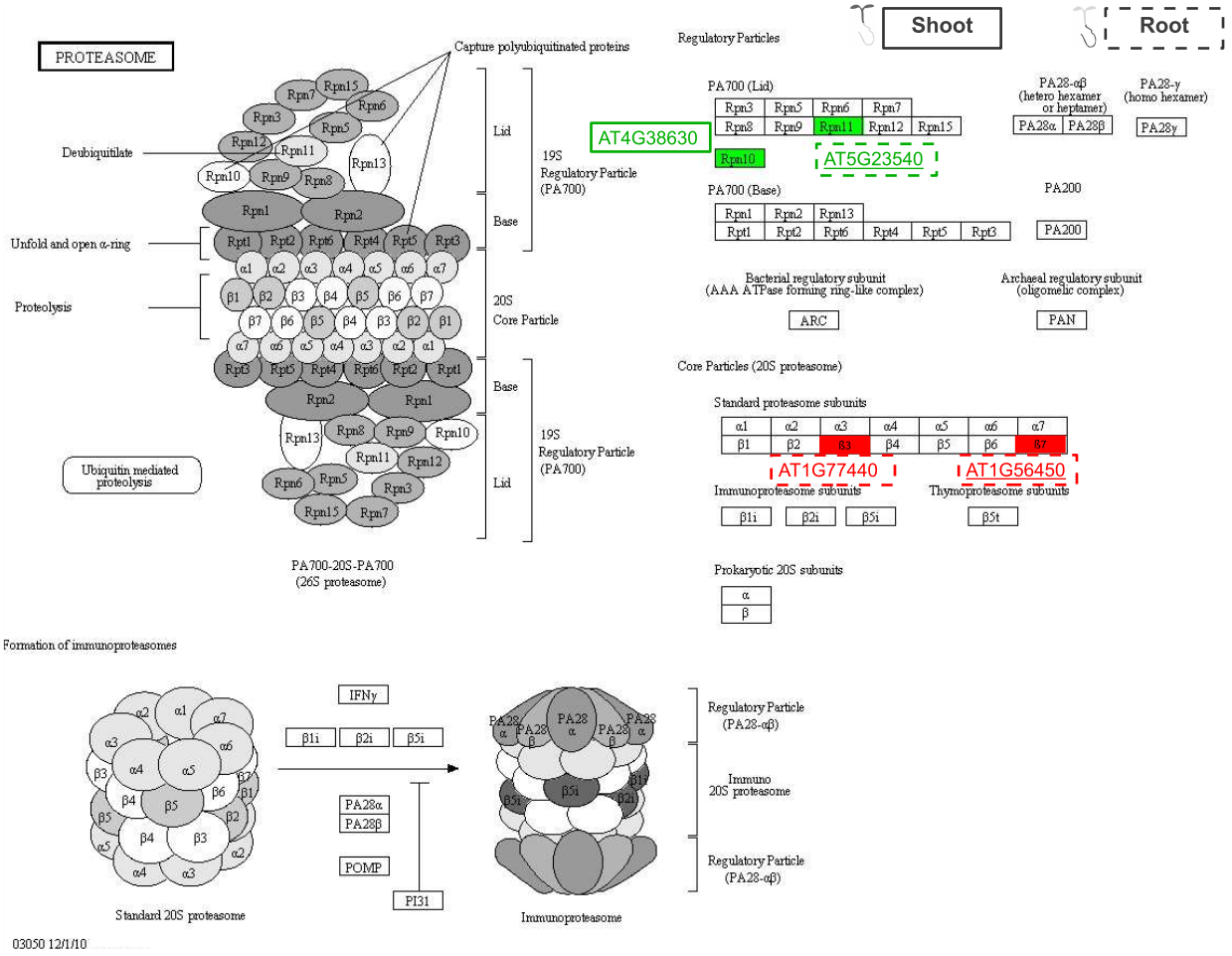
PROTEASOME
Capture polyubiquitinated proteins
Deubiquitilate
Unfold and open α-ring
Proteolysis
Ubiquitin mediated proteolysis
Lid
Base
19S Regulatory Particle (PA700)
20S Core Particle
PA700-20S-PA700 (26S proteasome)
Regulatory Particles
Shoot
Root
AT4G38630
AT5G23540
PA700 (Lid)
PA700 (Base)
PA28-αβ (hetero hexamer or heptamer)
PA28-γ (homo hexamer)
PA200
Bacterial regulatory subunit (AAA ATPase forming ring-like complex)
Archaeal regulatory subunit (oligomeric complex)
ARC
PAN
Core Particles (20S proteasome)
Standard proteasome subunits
AT1G77440
AT1G56450
Immunoproteasome subunits
Thymoproteasome subunits
Prokaryotic 20S subunits
Formation of immunoproteasomes
IFNγ
PA28α
PA28β
POMP
PI31
Standard 20S proteasome
Immunoproteasome
Regulatory Particle (PA28-αβ)
Immuno 20S proteasome
Regulatory Particle (PA28-αβ)
03050 12/1/10

C

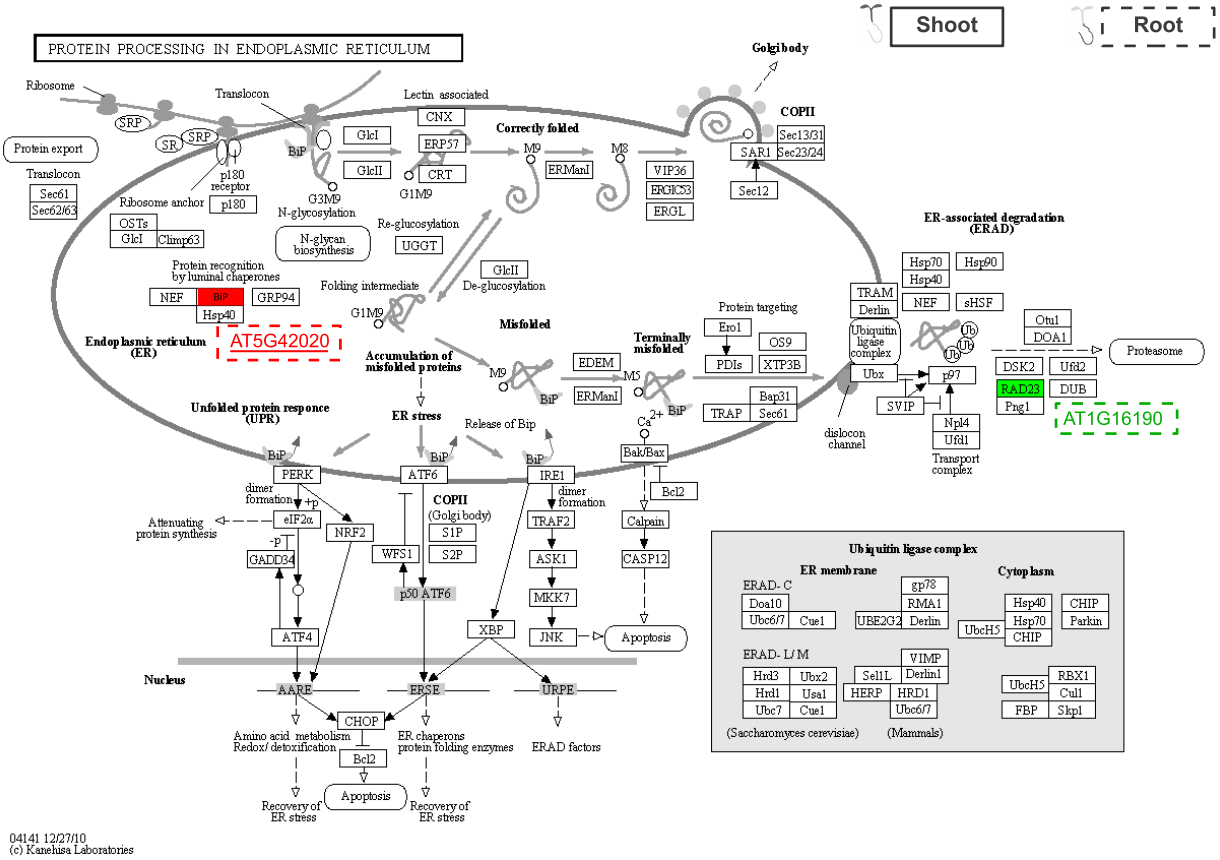
Shoot
Root
PROTEIN PROCESSING IN ENDOPLASMIC RETICULUM
Golgi body
Ribosome
Translocon
Lectin associated
CNX
COPII
SRP
SR
Protein export
Translocon
Sec61
Sec62/63
p180 receptor
p180
Ribosome anchor
OSTs
Glc1
Climp63
BiP
Glc1
GlcII
ERP57
CRT
G3M9
G1M9
N-glycosylation
Correctly folded
M9
M8
ERManI
VIP36
ERGIC53
ERGL
SAR1
Sec13/31
Sec23/24
Sec12
N-glycan biosynthesis
Re-glucosylation
UGGT
GlcII
De-glucosylation
Protein recognition by luminal chaperones
NEF
BiP
GRP94
Hsp40
Folding intermediate
G1M9
Endoplasmic reticulum (ER)
AT5G42020
Misfolded
Accumulation of misfolded proteins
EDEM
ERManI
M5
M9
BiP
Terminally misfolded
Protein targeting
Ero1
PDIs
OS9
XTP3B
TRAP
Bap31
Sec61
ER-associated degradation (ERAD)
Hsp70
Hsp90
Hsp40
NEF
sHSF
TRAM
Derlin
Ubiquitin ligase complex
Ub
Ubx
p97
SVIP
Npl4
Ufd1
Transport complex
dislocon channel
Otu1
DOA1
DSK2
Ufd2
RAD23
DUB
Png1
Proteasome
AT1G16190
Unfolded protein responce (UPR)
ER stress
Release of Bip
Ca2+
Bak/Bax
Bcl2
PERK
ATF6
IRE1
dimer formation
+P
eIF2α
-P
Attenuating protein synthesis
NRF2
GADD34
ATF4
WFS1
COPII
(Golgi body)
S1P
S2P
p50 ATF6
TRAF2
ASK1
MKK7
JNK
XBP
Calpain
CASP12
Apoptosis
Nucleus
AARE
ERSE
URPE
CHOP
Amino acid metabolism
Redox/ detoxification
ER chaperons
protein folding enzymes
ERAD factors
Bcl2
Apoptosis
Recovery of ER stress
Recovery of ER stress
Ubiquitin ligase complex
ER membrane
Cytoplasm
ERAD- C
Doa10
Ubc6/7
Cue1
gp78
RMA1
UBE2G2
Derlin
UbcH5
Hsp40
Hsp70
CHIP
CHIP
Parkin
ERAD- L/ M
Hrd3
Ubx2
Hrd1
Usa1
Ubc7
Cue1
VIMP
Sel1L
Derlin1
HERP
HRD1
Ubc6/7
UbcH5
RBX1
Cul1
FBP
Skp1
(Saccharomyces cerevisiae)
(Mammals)
04141 12/27/10
(c) Kanehisa Laboratories

D

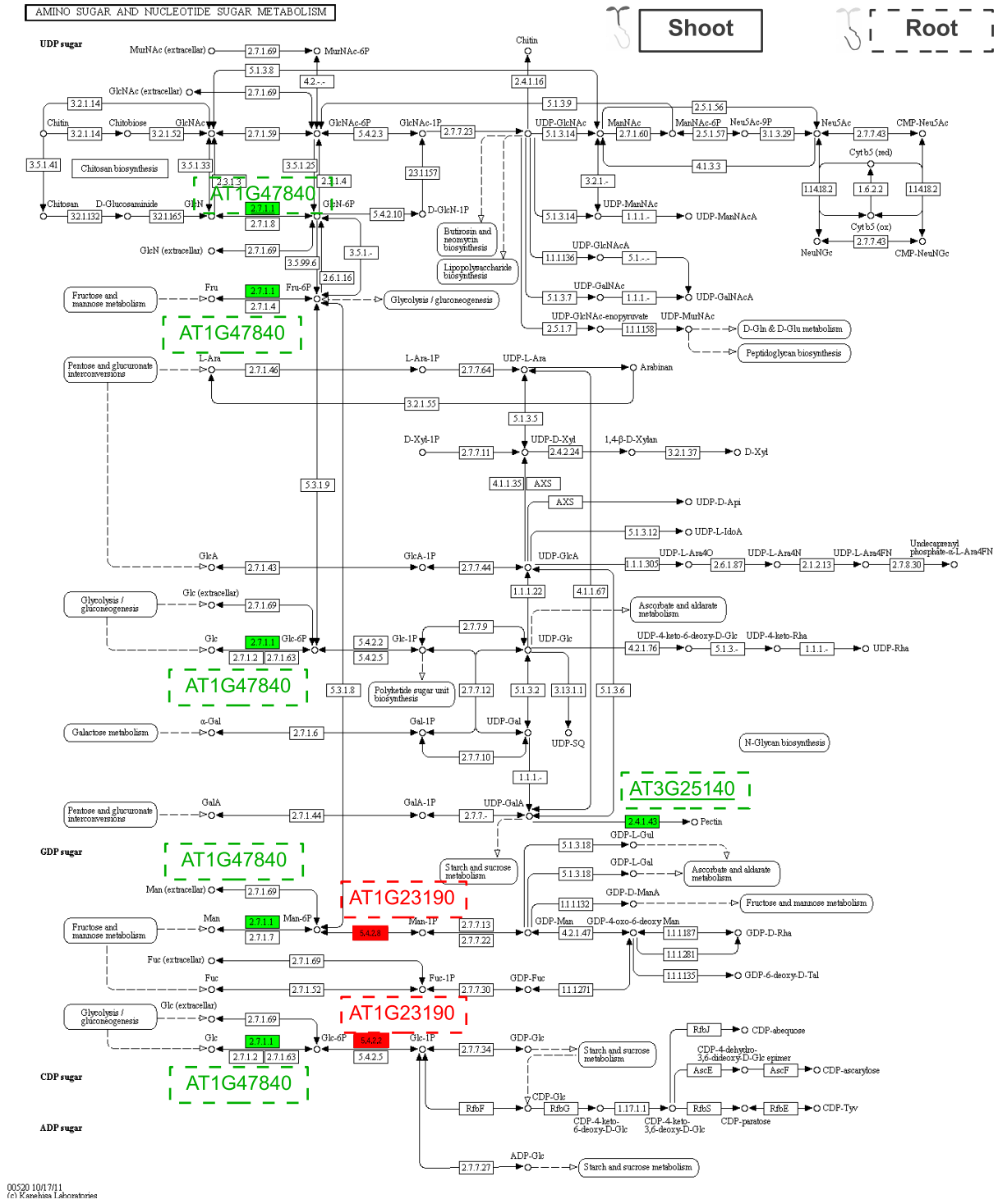
AMINO SUGAR AND NUCLEOTIDE SUGAR METABOLISM
Shoot
Root
AT1G47840
AT1G47840
AT1G47840
AT1G47840
AT1G47840
AT3G25140
AT1G23190
AT1G23190
UDP sugar
GDP sugar
CDP sugar
ADP sugar
Chitosan biosynthesis
Fructose and mannose metabolism
Glycolysis / gluconeogenesis
Pentose and glucuronate interconversions
Galactose metabolism
Starch and sucrose metabolism
Ascorbate and aldarate metabolism
N-Glycan biosynthesis
Peptidoglycan biosynthesis
Lipopolysaccharide biosynthesis
Polyketide sugar unit biosynthesis
Butirosin and neomycin biosynthesis
D-Gln & D-Glu metabolism
Arabinan
Pectin
00520 10/17/11
(c) Kanehisa Laboratories

E

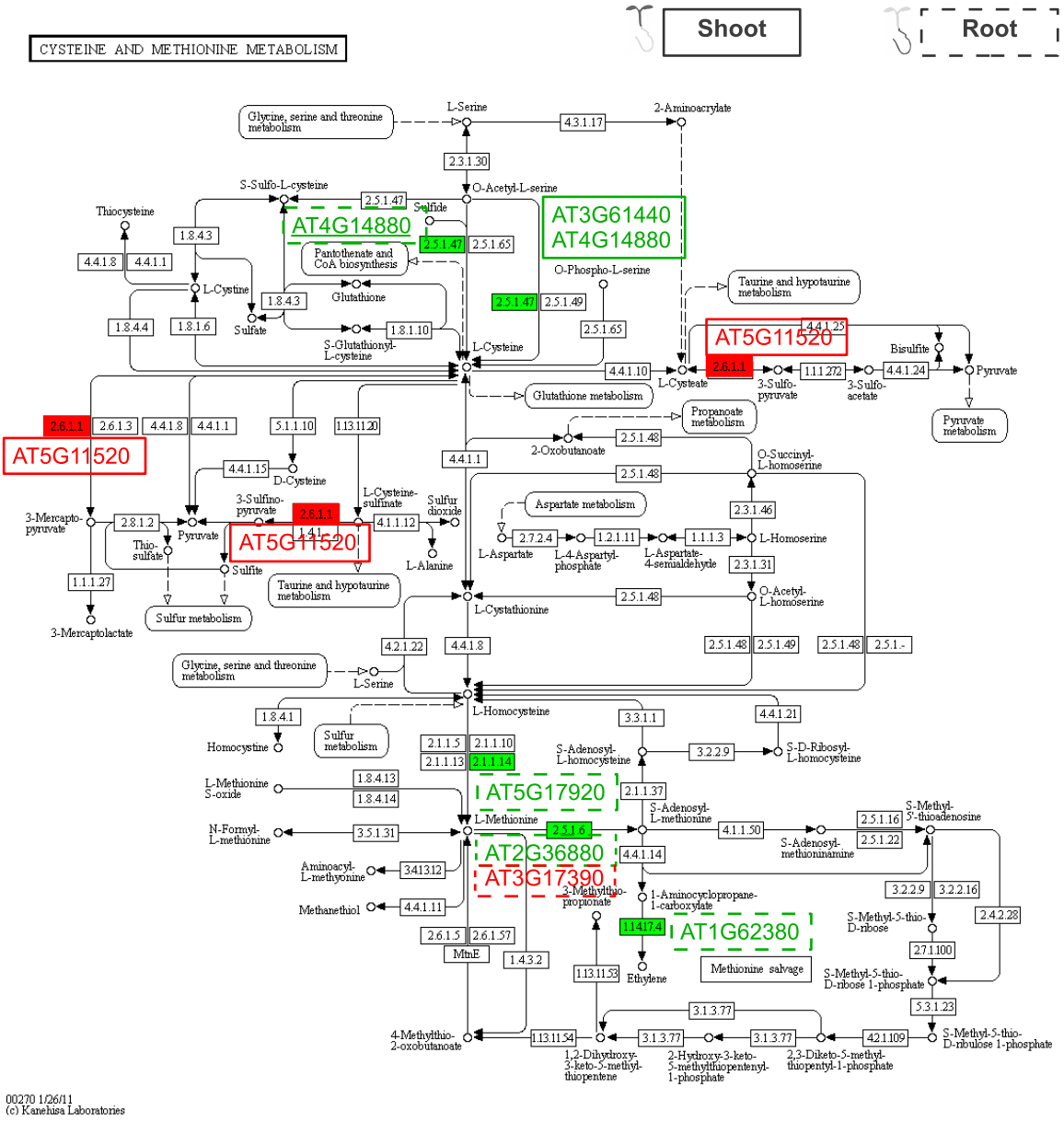
Shoot
Root
CYSTEINE AND METHIONINE METABOLISM
AT4G14880
AT3G61440
AT4G14880
AT5G11520
AT5G11520
AT5G11520
AT5G17920
AT2G36880
AT3G17390
AT1G62380
Glycine, serine and threonine metabolism
L-Serine
2-Aminoacrylate
S-Sulfo-L-cysteine
O-Acetyl-L-serine
Thiocysteine
Selfide
Pantothenate and CoA biosynthesis
L-Cystine
Glutathione
Sulfate
S-Glutathionyl-L-cysteine
L-Cysteine
O-Phospho-L-serine
Taurine and hypotaurine metabolism
Bisulfite
Pyruvate
L-Cysteate
3-Sulfo-pyruvate
3-Sulfo-acetate
Glutathione metabolism
Propanoate metabolism
Pyruvate metabolism
2-Oxobutanoate
O-Succinyl-L-homoserine
D-Cysteine
3-Sulfino-pyruvate
L-Cysteine-sulfinate
Sulfur dioxide
Aspartate metabolism
L-Aspartate
L-4-Aspartyl-phosphate
L-Aspartate-4-semialdehyde
L-Homoserine
3-Mercapto-pyruvate
Thio-sulfate
Sulfite
L-Alanine
O-Acetyl-L-homoserine
L-Cystathionine
3-Mercaptolactate
Sulfur metabolism
Taurine and hypotaurine metabolism
Glycine, serine and threonine metabolism
L-Serine
L-Homocysteine
Homocystine
Sulfur metabolism
S-Adenosyl-L-homocysteine
S-D-Ribosyl-L-homocysteine
L-Methionine S-oxide
L-Methionine
S-Adenosyl-L-methionine
S-Methyl-5'-thioadenosine
N-Formyl-L-methionine
S-Adenosyl-methioninamine
Aminoacyl-L-methyonine
3-Methylthio-propionate
1-Aminocyclopropane-1-carboxylate
Methanethiol
S-Methyl-5-thio-D-ribose
Ethylene
Methionine salvage
MtnE
S-Methyl-5-thio-D-ribose 1-phosphate
4-Methylthio-2-oxobutanoate
1,2-Dihydroxy-3-keto-5-methyl-thiopentene
2-Hydroxy-3-keto-5-methylthiopentenyl-1-phosphate
2,3-Diketo-5-methyl-thiopentyl-1-phosphate
S-Methyl-5-thio-D-ribulose 1-phosphate
00270 1/26/11
(c) Kanehisa Laboratories

Supplemental Figure 3. BAP regulates proteins involved in phytohormone biosynthesis. Proteins regulated in the shoot are framed within continuous lines, whereas those regulated in the root are framed within dashed lines. **Down-regulated** proteins are indicated in red and **up-regulated** ones in green. Proteins that are upregulated or downregulated after 120 minutes (delayed response) are underlined. Stars indicate proteins that were found in mixed spots on the 2-D gels. Proteins were mapped using the *Arabidopsis thaliana* KEGG Pathway tool and the background map was modified from the *Arabidopsis thaliana* 'Hormone biosynthesis pathways' map in KEGG (Ogata et al., 1999).

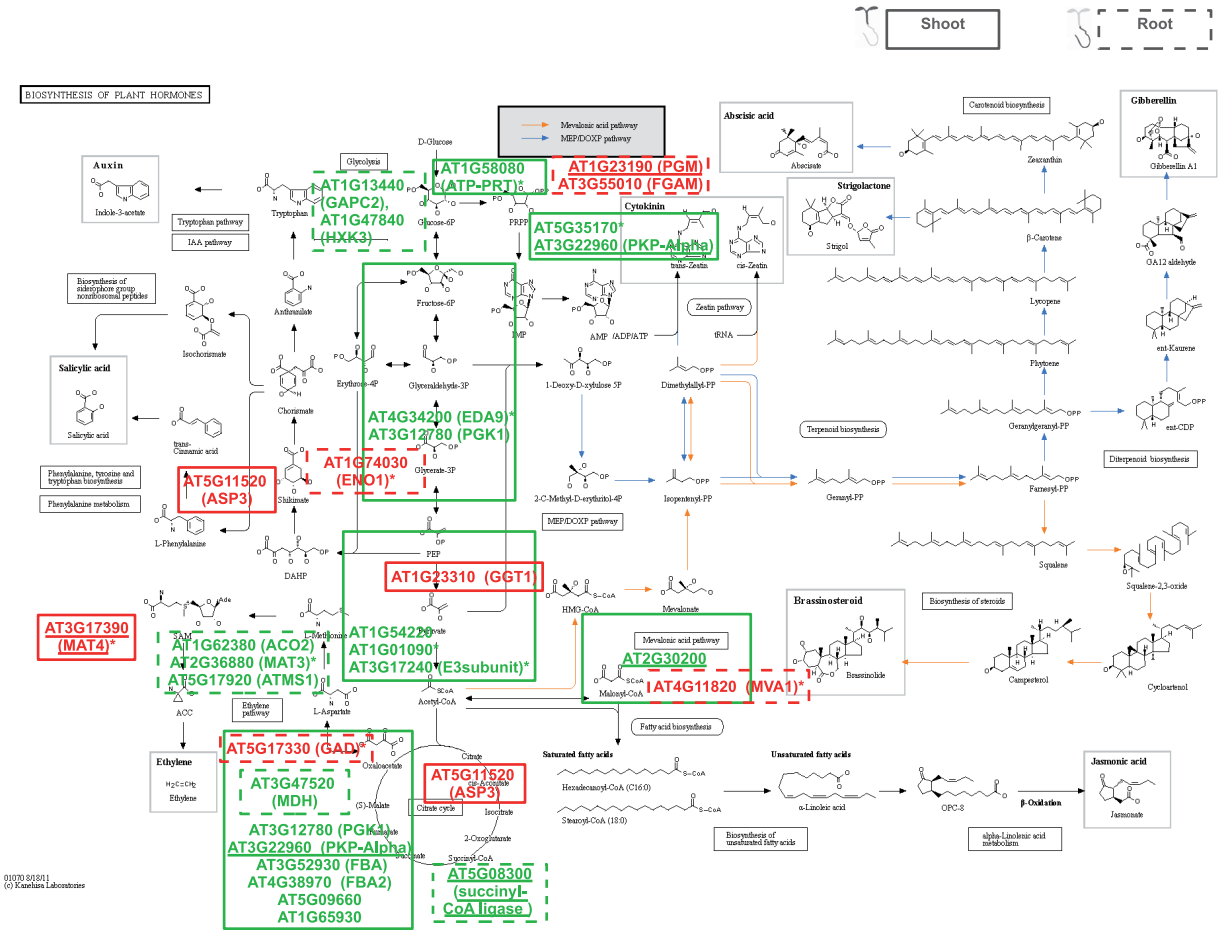

Supplemental Figure 4. Exogenous BAP application modulates levels of endogenous CKs and their metabolites. tZ, trans-zeatin; cZ; cis-zeatin; DHZ, dihydrozeatin; iP, isopentenyladenine; BAP, 6-benzylaminopurine; mT; meta-topolin; oT, ortho-topolin; pT, para-topolin. In all abbreviations, “R” correspond to ribosides, “OG” to O-glucosides, “ROG“ to O-glucoside ribosides, “9G” to N-9-glucosides, and R-“5'MP” to riboside 5´monophosphates. Levels of DHZ, DHZOG, mTOG, mTROG, oTR, oTOG, oTROG, oTR-5'MP were below detection limits, and therefore their respective charts are excluded. The statistical significance of differences between mock(-)- and BAP(+)-treated samples (t test) at alpha=0.05, 0.01, and 0.001 is denoted by *, **, and ***, respectively, and shown above of the respective bars. Error bars indicate standard deviations.

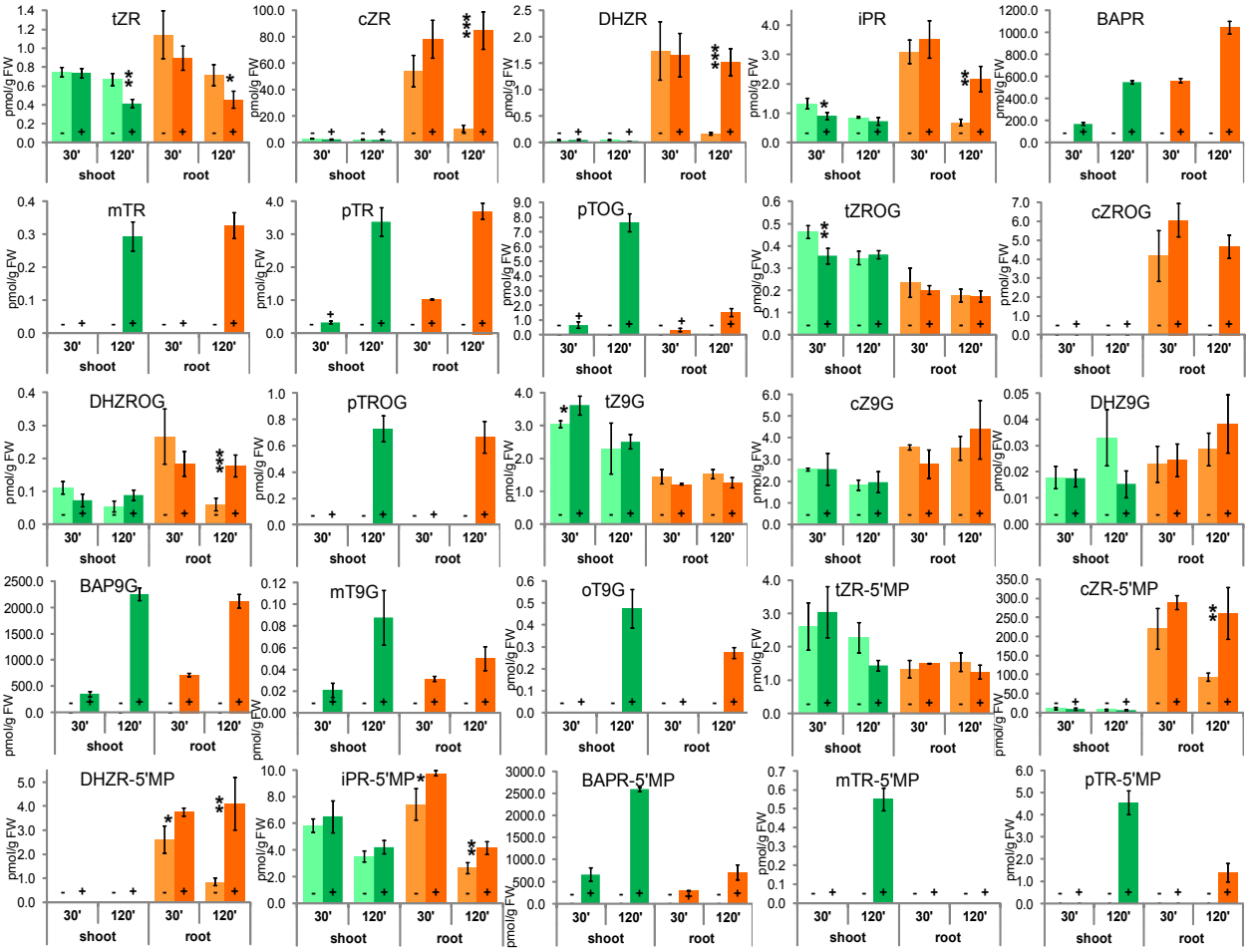

Supplemental Figure 5. Typical 2-DE maps showing the quality of gel separation. Figures A-D represent four biological replicas of shoot samples treated with 5 µM BAP for 30 min. 150 micrograms of protein was applied to 18 cm long IPG strips (nonlinear pH gradient, pH 3-10), 12% SDS-PAGE gels were used in the second dimension and fluorescent SYPRO Ruby stain was employed for the protein detection.

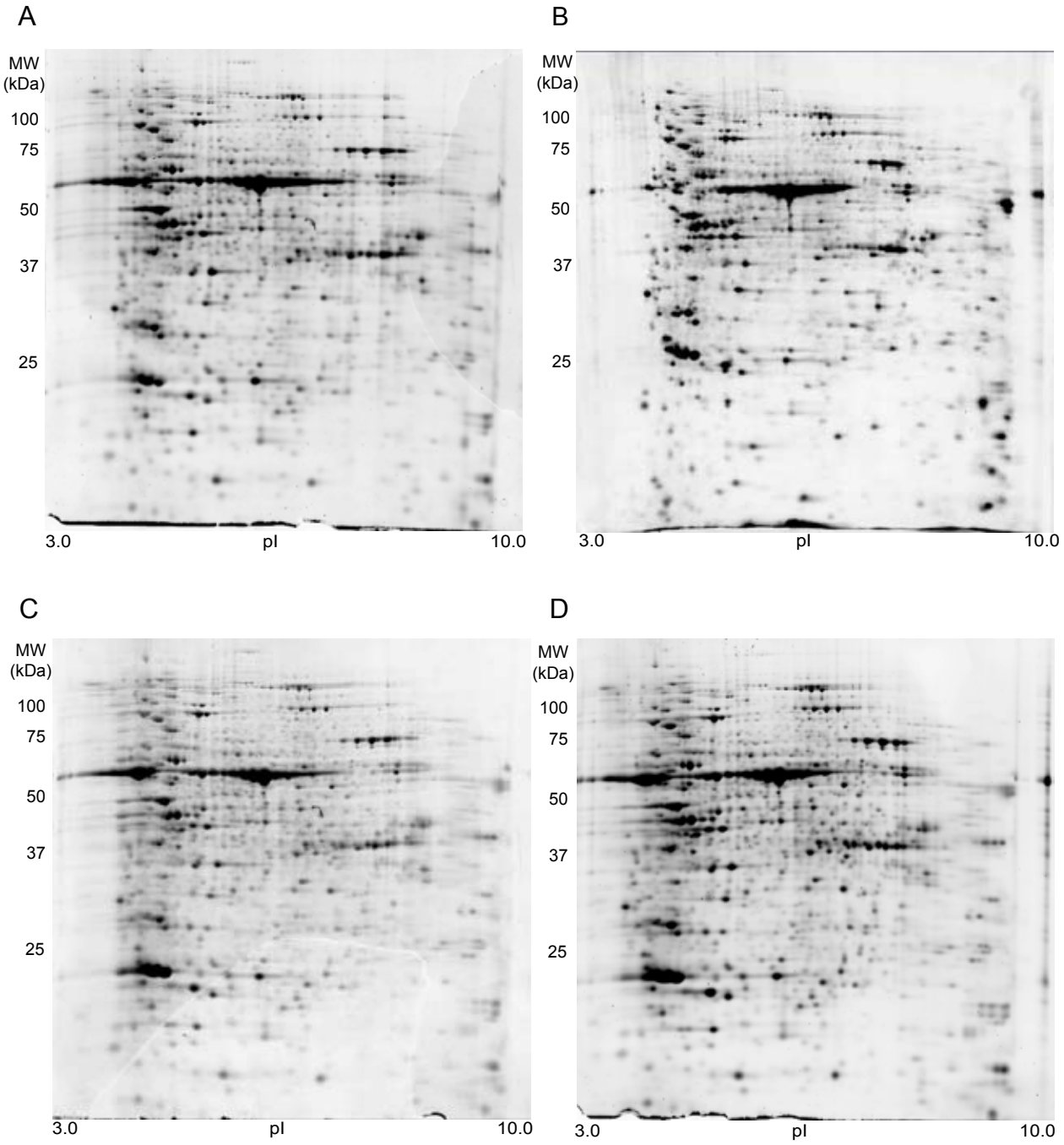

Supplemental Figure 6. Root apical meristem lengths and root cell lengths of mutants in ethylene biosynthesis in a response to BAP. The statistical significance of differences identified between mock- and BAP-treated plants (2 days of incubation) using t test at alpha=0.05, 0.01 and 0.001 is denoted by *, ** and ***, respectively.

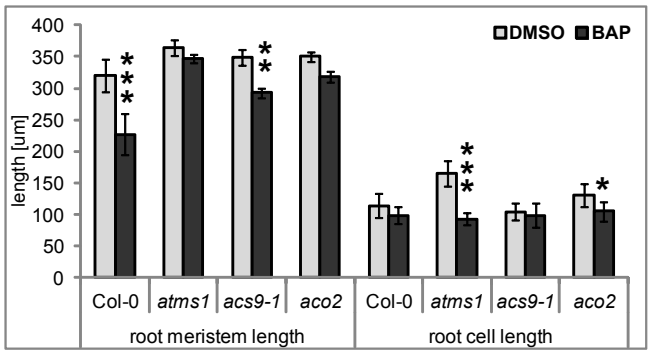

Supplemental Figure 7. BAP-mediated ethylene production in ethylene-responsive reporter line EBS:GUS in the shoot (A) and root (B).

A

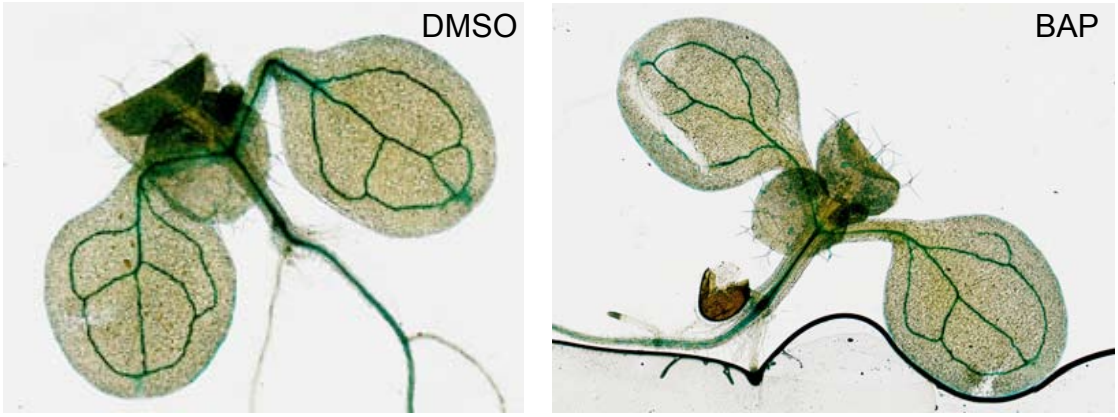

B

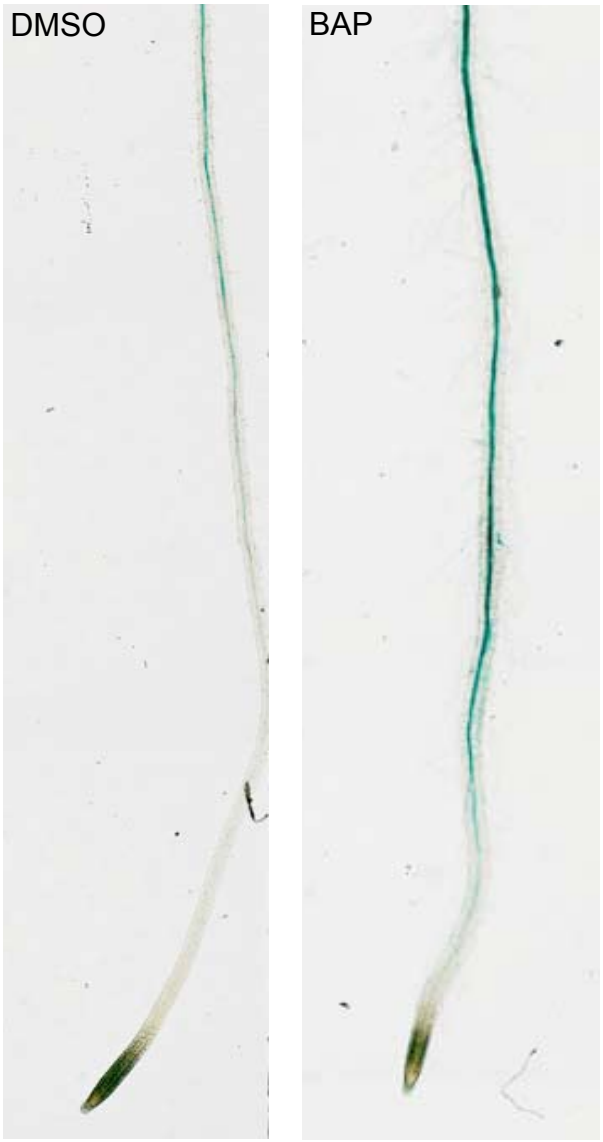

Supplemental Table 1. BAP-regulated proteins in Arabidopsis seedlings. This table demonstrates the list of proteins successfully identified from excised spots.

Proteins that were up- or down-regulated after BAP treatment were categorized according to the tissue in which the difference was found (shoot or root) and according to the response type: qualitative (Supplemental Table 1A) or quantitative (Supplemental Table 1B). **30' up, 120' none** are proteins upregulated after 30 min of BAP treatment but revealing no change after 120 min. **30' down, 120' none** are proteins downregulated after 30 min of BAP treatment but revealing no change after 120 min. Accordingly, **30' none, 120' up** are proteins revealing no change after 30 min but being upregulated after 120 min of BAP treatment and **30' none, 120' down** are proteins revealing no change after 30 min but being downregulated after 120 min of BAP treatment.

"**SSP #**" stands for spot-specific number assigned by PDQuest 2-D Analysis Software Version 8.0.1, used for image analysis. Annotated functions of proteins were classified according to the functional catalogue of plant genes established previously (Bevan et al., 1998). In case of protein classification into multiple functional categories a single category was selected as based on experimental evidence currently available. The color code of functional categories corresponds to the color code used in Figures 1A and 1B. Proteins in red font are stress-related and underlined proteins are related to cold or heat response. Scores in **bold font** are for proteins identified by two or more peptides with statistically significant individual score ($p < 0.05$; MASCOT peptide score 45 or higher). Scores in normal font are for proteins identified only by one peptide with statistically significant individual score.

Identified proteins showing **qualitative** changes (i.e. spots present or absent when compared with the control) are listed in **Supplemental Table 1A**.The spot intensity 10-fold higher as compared to gel background was considered as qualitatively significant. All proteins involved in multiple protein identifications in single spots were considered for qualitative evaluation.

For quantitative differentiation, 1.5-fold change or higher was regarded as significant (average normalized spot intensity between compared samples). Statistical significance of differences was assessed using t test. Proteins identified in **quantitatively** different spots ($p < 0.05$) are listed in **Supplemental Table 1B**. For quantification only proteins from spots with single identified protein were considered.

Supplemental Table 1A

	Category of expression change, QUALITY	SSP #	AGI code	Protein name	Expected function	LC-MS/MS Score	LC-MS/MS % Cov	LC-MS/MS peptide No.	MW (kDa)	pI
SHOOT	30' up, 120' none	1443	AT4G20360	Arabidopsis Rab GTPase homolog E1b (ATRABE1B)	Protein synthesis	220	13	7	51,6	5,8
		1542	AT3G13235	ubiquitin family protein - DNA-damage inducible 1 (DDI1)	Protein destination and storage	329	16	9	45,3	4,8
			AT5G16620	pigment defective embryo (PDE120)	Transporters	272	16	6	58,9	5,4
			AT3G12780	phosphoglycerate kinase 1 (PGK1)	Energy	250	18	8	50,1	5,9
		1879	AT4G24190	shepherd (SHD)	Protein destination and storage	868	26	21	94,1	4,9
		2859	AT3G29320	alpha-glucan phosphorylase 1 (PHS1)	Metabolism	282	12	16	108,5	5,3
			AT4G33010	P-Protein - like protein	Metabolism	70	4	4	112,9	6,5
		3533	AT1G54220	dihyrdolipoamide acetyltransferase	Metabolism	185	8	4	56,3	8,3
		3862	AT2G40840	4-alpha-glucanotransferase	Metabolism	107	7	8	109,7	5,5
		3926	AT3G48110	glycyl-tRNA synthetase	Transcription	62	2	3	119,8	5,7
		4431	AT1G01090	pyruvate dehydrogenase	Energy	197	17	8	47,1	7,2
			AT1G58080	ATP phosphoribosyl transferase	Metabolism	123	10	4	44,5	6,0
			AT1G80600	HOPW1-1-interacting 1 (WIN1)	Disease/defense	105	8	4	48,8	6,3
			AT5G54160	O-methyltransferase 1 (OMT1)	Metabolism	73	5	2	39,6	5,6
		4634	AT4G34200	embryo sac development arrest 9 (EDA9)	Cell growth/division	78	6	5	63,3	5,6
			ATCG00490	ribulosebisphosphate carboxylase	Energy	77	5	3	47,6	5,6
			AT1G05180	auxin resistant 1 (AXR1)	Protein destination and storage	60	6	4	60,0	5,6
		5655	AT2G07698	ATP synthase subunit alpha, mitochondrial	Transporters	174	23	15	55,0	5,6
			AT5G35170	adenylate kinase family protein	Energy	145	17	10	65,7	5,6
			AT3G17240	2-oxoglutarate dehydrogenase, E3 subunit	Energy	144	13	6	50,0	5,6
			AT5G52520	ovule abortion 6 (OVA6)	Transcription	121	5	3	60,7	5,6
			ATCG00490	ribulosebisphosphate carboxylase	Energy	116	8	4	47,6	5,6
		7347	AT3G61440	beta-substituted ala synthase 3 (ATCYSC1)	Metabolism	219	20	7	39,9	5,6
		8264	AT5G09660	malat dehydrogenase	Energy	332	26	10	37,3	5,6
	30' down, 120' none	5542	AT1G23310	aminotransferase 1 (GGT1)	Energy	93	12	8	53,3	6,9
		6822	AT1G68560	alpha-xylosidase precursor	Metabolism	79	3	4	101,9	6,3
		7516	AT3G02360	6-phosphogluconate dehydrogenase family protein	Energy	115	8	5	53,5	7,0
		8014	ATCG00130	ATP synthase CF0 B subunit	Transporters	190	31	6	21,0	7,9
		8440	AT1G30580	GTP binding	Energy	99	15	7	44,4	6,4
		9406	AT5G11520	asparate aminotransferase 3 (ASP3)	Metabolism	222	20	10	49,0	9,3
	30' none, 120' up	1425	AT5G45930	magnesium chelatase subunit of protochlorophyllide reductase	Energy	310	22	12	46,5	5,2
		1871	AT2G32240	At2g32240/F22D22.1	Unclear classification	88	12,9	8	63,0	4,8
		3234	AT2G30200	[acyl-carrier-protein] S-malonyltransferase (EMB3147)	Metabolism	100	2,8	1	41,5	9,4
		4447	AT3G48730	glutamate-1-semialdehyde aminotransferase	Metabolism	104	7,2	3	50,1	8,6
		9225	AT2G45820	DNA-binding protein	Cell growth/division	53	2,9	1	21,0	7,9
	30' none, 120' down	1042	ATCG00490	ribulose-1,5-bisphosphate carboxylase large subunit (RBCL)	Energy	75	9	6	53,0	5,9
		4344	AT4G36530	hydrolase, alpha/beta fold family protein	Metabolism	78	7	4	41,9	7,6
		4433	AT5G63570	glutamate-1-semialdehyde 2,1-aminomutase (GSA1)	Metabolism	104	7	3	50,3	6,4
		4546	AT3G17390	methionine adenosyltransferase (MTO3, MAT4)	Metabolism	88	4	2	42,8	5,5
			AT3G22890	ATP sulfurylase 1 (APS1)	Metabolism	87	9	5	51,4	6,3
		7616	AT1G63660	GMP synthase	Metabolism	162	18	12	59,3	6,1
		8388	AT1G29670	GDSL-motif lipase/hydrolase family protein	Metabolism	252	14	4	39,8	8,9
ROOT	30' up, 120' none	0506	AT1G16190	DNA repair protein RAD23, putative	Protein destination and storage	392	17	7	39,8	4,4
			AT3G26380	alpha-galactosidase-like protein (F20C19.10)	Metabolism	320	17	6	48,0	4,7
		0814	AT1G56070	translation elongation factor (LOS1)	Protein synthesis	840	26	18	93,8	5,6
		1216	AT1G62380	ACC oxidase 2 (ACO2)	Metabolism	305	15	4	36,1	5,0
		1315	AT1G10840	eukaryotic initiation factor 3H1 subunit	Protein synthesis	246	16	6	38,3	4,8
		1903	AT5G07350	tudor-sn protein 1 (TUDOR1)	Protein synthesis	1133	23	21	108,2	6,1
		2215	AT3G55000	tonneau 1 (TON1)	Cell structure	198	13	4	29,3	5,4
		2617	AT3G03960	putative T-complex protein 1,theta subunit (TCP-1-Theta)	Protein destination and storage	1010	37	16	56,9	5,3
		3425	AT3G47520	malat dehydrogenase (MDH)	Energy	121	7	2	42,4	8,5
		3516	AT1G65220	eIF4-gamma domain-contain. protein	Protein synthesis	492	19	7	47,2	5,5
			AT2G36880	S-adenosylmethionine transferase 3 (MAT3)	Metabolism	301	20	7	42,8	5,5
		5223	AT5G20020	RAS-related GTP-binding nuclear protein 2 (RAN2)	Protein destination and storage	109	9	2	25,0	6,7
		5902	AT5G07350	tudor-sn protein 1 (TUDOR1)	Transcription	944	20	16	107,7	6,2
		6531	AT1G47840	hexokinase 3 (HXK3)	Signal transduction	68	1	1	96,9	6,3
		7126	AT5G13450	delta subunit of mitochondrial F1-ATPase (ATP5)	Transporters	179	16	3	26,2	9,4
			AT1G14410	A. thaliana Whirly 1 (ATWHY1/PTAC1)	Cell growth/division	126	11	2	29,0	9,4
		7519	AT5G60390	elongation factor 1-alpha (EF-1-alpha)	Protein synthesis	274	13	7	49,4	9,2
		7521	AT5G60390	elongation factor 1-alpha (EF-1-alpha)	Protein synthesis	198	12	5	49,4	9,2
		8525	AT5G60390	elongation factor 1-alpha (EF-1-alpha)	Protein synthesis	288	21	8	49,4	9,2
		8615	AT1G47600	beta glucosidase34 (BGLU34)	Metabolism	114	4	3	57,5	8,3
	30' down, 120' none	1813	AT3G55010	phosphoribosylformylglycinamidine synthase (FGAM)	Metabolism	50	1,6	2	151,7	5,6
		2127	AT1G77440	putative 20S proteasome beta subunit C2 (PBC2)	Protein destination and storage	147	17,8	4	21,4	5,8
		3418	AT5G08690	mitochondrial F1 ATP synthase beta subunit	Transporters	446	18,3	11	63,3	6,6
			AT5G17330	glutamate decarboxylase (GAD)	Metabolism	348	25,9	18	57,1	5,2
			AT1G74030	phosphopyruvate enolase (ENO1)	Metabolism	292	23,4	10	47,7	5,5
		5315	AT2G44350	citrat synthase 4 (ATCS)	Energy	183	12,3	9	52,6	6,4
			AT4G11820	hydroxymethylglutaryl-CoA synthase (MVA1)	Metabolism	172	13,4	8	51,1	6,0
		5710	AT3G16460	mannose-binding lectin superfamily protein (T2O4.14)	Disease/defense	415	16,9	11	72,4	5,2
	30' none, 120' up	8411	AT3G25140	galacturonosyltransverase 8 (GAUT8)	Metabolism	55	2,1	1	64,3	9,4
		8412	AT4G00660	RNA helicase-like 8 (RH8)	Protein synthesis	91	11,1	5	57,6	9,2
		8413	AT1G76160	SKU5 Similar 5 (SKS5)	Metabolism	178	10,9	7	60,0	9,0
		8511	AT3G46740	translocon outer membrane complex 75-III (TOC75-III)	Transporters	311	11,5	9	89,1	9,5
			AT1G49760	poly(A) binding protein 8 (PAB8)	Protein synthesis	72	3,6	2	49,9	9,7
		9103	AT3G62830	UDP-glucuronic acid decarboxylase 2 (UXS2)	Metabolism	164	16,4	5	49,9	9,7
		9104	AT2G02400	cinnamoyl-CoA reductase family (CCRfam)	Metabolism	74	6,9	3	35,6	9,3
	30' none, 120' down	3124	AT2G26670	heme Oxygenase 1 (HO1)	Energy	103	11	3	28,0	5,6
		3514	AT1G23190	glucose phosphomutase, putative (PGM)	Metabolism	703	29	14	63,4	5,6
		4337	AT4G29210	gamma-glutamyltransferase 3 (GGT3)	Disease/defense	137	5	3	69,1	5,8

Supplemental Table 1B

	Category of expression change, QUANTITY	SSP #	Relative abundance	P-values	AGI code	Protein name	Expected function	LC-MS/MS			MW (kDa)	pI
									% Cov	peptide No.		
SHOOT	30' up, 120' none	2225	3,8	0,02	AT3G16420	PYK10-binding protein 1 (PBP1)	Protein destination and storage	209	24	7	32,1	5,5
		2411	3,4	0,01	AT3G12780	phosphoglycerate kinase 1 (PGK1)	Energy	268	13	7	50,1	5,9
		5021	2,2	0,05	AT5G20630	Arabidopsis thaliana germin 3 (ATGER3)	Cell structure	100	9	3	21,8	6,8
		5155	2,1	0,05	AT2G47730	glutathione S-transferase (GST6)	Disease/defense	280	45	10	24,1	6,1
		5306	7,7	0,05	AT4G14880	cysteine synthase (OASA1)	Metabolism	321	25	7	33,8	5,7
		5307	4,4	0,05	AT4G38970	fructose-bisphosphate aldolase (FBA2)	Metabolism	344	23	9	43,0	6,8
		6320	4,0	0,02	AT3G52930	fructose-bisphosphate aldolase, putative (FBA)	Metabolism	166	16	6	38,5	6,1
		6413	3,0	0,02	AT1G65930	cytosolic NADP+ dependent isocitrate dehydrogenase (cICDH)	Energy	611	48	22	45,7	6,1
		6418	4,8	0,05	AT3G52880	monodehydroascorbate reductase 1 (ATMDAR1)	Metabolism	202	23	9	46,5	6,4
		7207	1,8	0,04	ATCG00540	cytochrome f	Energy	162	16	5	35,3	8,3
		7303	1,7	0,03	AT3G52930	fructose-bisphosphate aldolase, putative (FBA)	Metabolism	386	33	13	38,5	6,1
		7413	2,5	0,04	AT1G68010	hydroxypyruvate reductase (ATHPR1, HPR)	Energy	150	9	4	42,3	7,1
		8024	2,5	0,05	AT4G28520	cruciferin 3 (CRU3)	Cell growth/division	199	12	6	58,2	6,5
	30' none, 120' up	0306	1,7	0,05	AT4G35450	ankyrin repeat-containing protein 2 (AKR2)	Disease/defense	311	23	8	36,9	4,5
		1521	2,1	0,04	AT4G38630	regulatory particle non-ATPase 10 (RPN10)	Signal transduction	435	24	12	40,7	4,5
		2721	1,9	0,04	AT3G22960	pyruvate kinase (PKP-Alpha)	Energy	366	24	15	65,1	5,6
		9211	2,2	0,02	AT5G26280	MATH domain-containing protein	Unclear classification	117	20	7	39,4	8,5
	30' none, 120' down	4406	0,4	0,04	AT4G20360	Arabidopsis Rab GTPase homolog E1b (ATRABE1B)	Protein synthesis	607	29	6	51,6	5,6
		5208	0,4	0,05	AT1G07890	ascorbate peroxidase 1 (APX1)	Disease/defense	138	22	7	27,5	5,7
ROOT	30' up, 120' none	5714	3,5	0,01	AT5G17920	cobalamine independent methionine synthase (ATMS1)	Metabolism	301	19	20	84,3	6,1
		8011	1,5	0,01	AT5G15090	voltage anion channel 3 (VDAC3)	Transporters	352	33	12	29,2	7,9
	30' down, 120' none	3216	0,2	0,05	AT1G14170	KH domain-containing protein NOVA, putative	Transcription	275	22,7	6	33,8	5,6
	30' none, 120' up	3002	1,6	0,03	AT2G21660	cold, circadian rhythm, and RNA binding 2 (CCR2)	Transcription	564	64	12	16,9	5,9
		3128	1,9	0,05	AT4G14880	cysteine synthase (OASA1)	Metabolism	108	6	2	33,8	5,7
		5128	2,3	0,03	AT1G13440	glyceraldehyde-3-phosphate dehydrogenase C2 (GAPC2)	Energy	122	16	6	36,9	6,7
		5327	8,6	0,01	AT5G23540	26S proteasome regulatory subunit, putative (26S)	Protein destination and storage	360	22	6	34,3	6,3
		6022	1,8	0,05	AT3G27890	NADPH:quinone oxidoreductase (NQR)	Energy	120	17	4	21,5	6,8
		6822	2,0	0,05	AT5G22610	F-box family protein	Protein destination and storage	48	1,9	1	53,8	5,7
		7118	1,5	0,02	AT5G40770	prohibitin 3 (ATPHB3)	Disease/defense	237	31	10	30,4	7,0
		8217	1,5	0,04	AT5G08300	succinyl-CoA ligase	Metabolism	132	12	6	36,1	8,6
		8416	1,8	0,04	AT3G18190	TCP-1/cpn60 chaperoninfamily protein, putative (MRC8.2)	Protein destination and storage	68	5	4	57,7	7,6
	30' none, 120' down	2718	0,1	0,05	AT5G42020	luminal binding protein (BiP)	Protein destination and storage	311	17	14	73,4	5,1
		7003	0,3	0,05	AT1G56450	20S proteasome beta subunit G1 (PBG1)	Protein destination and storage	154	14	2	27,6	6,1

Supplemental Table 2. Overview of mapping BAP-regulated proteins in the KEGG database. Proteins regulated after 120 minutes of CK treatment are underlined; those regulated after 30 minutes of CK treatment are not. The function of proteins in bold has been confirmed experimentally in *Arabidopsis thaliana* (according to TAIR annotation, http://www.arabidopsis.org). Cellular localization according to the 'GO cellular component' annotation in TAIR is depicted. cl, chloroplast; cle, chloroplast envelope; cls, chloroplast stroma; pl, plastid; mit, mitochondrion; mitx, mitochondrial matrix; ap, apoplast; cw, cell wall; cp, cytoplasm; mem, plasma membrane; nuc, nucleus; thy, thylakoid; plg, plastoglobule; cyt, cytosol; mib, microbody; px, peroxisome; vac, vacuole; pd, plasmodesma; pr, proteasome; er, endoplasmic reticulum; gol, Golgi apparatus; all, present in all or almost all of these categories. Please note that the same protein can be involved in more than one process. The KEGG processes preferentially affected in the shoot are highlighted with light green colour and in the root with light orange colour.

KEGG Process family	KEGG Process and process number	Shoot Upregulated	Shoot Downregulated	Root Upregulated	Root Downregulated
Carbohydrate metabolism		(26)	(2)	(9)	(9)
	ath00010 Glycolysis / Gluconeogenesis	(7) **AT1G01090** – cl,cle,cls,pl **AT1G54220** - mit **AT3G12780** (PGK1) -all **AT3G17240** (E3) – cl,mit,mitx **AT3G22960** (PKP-Alpha) – cl,cls AT3G52930 (FBA) - all AT4G38970 (FBA2) – cl,cle,cls,mem,ap,thy,plg		(2) **AT1G13440** (GAPC2) - all AT1G47840 (HXK3) - cl	(2) AT1G23190 (PGM)– cl, nuc, mem, cyt, cp **AT1G74030** (ENO1) – cl, cls
	ath00020 Citrate cycle (TCA cycle)	(5) **AT1G01090** - cl,cle,cls,pl **AT1G54220** - mit AT1G65930 (cICDH) – ap, cls, cyt, pd, mem **AT3G17240** (E3)– cl,mit,mitx **AT5G09660** – ap, cl, cle, mib, px, vac		(2) **AT3G47520** (MDH) – ap, cl, cle, cls, mem, vac, mit AT5G08300	(1) AT2G44350 (ATCS) – cw, cl, mit
	ath00030 Pentose	(2) AT3G52930 (FBA) - all	(1) AT3G02360 – cls, cyt, px		(1) AT1G23190 (PGM) – cl, nuc,

	phosphate pathway	AT4G38970 (FBA2) – cl,cle,cls,mem,ap,thy,plg			mem, cyt, cp
	ath00051 Fructose and mannose metabolism	(2) AT3G52930 (FBA) - all AT4G38970 (FBA2) – cl,cle,cls,mem,ap,thy,plg			
	ath00052 Galactose metabolism			(1) AT1G47840 (HXK3) - cl	(1) AT1G23190 (PGM) – cl, cls, cp, cyt, nuc, mem
	ath00053 Ascorbate and aldarate metabolism	(1) **AT3G52880** (ATMDAR1) – ap, px, cl, pm	(1) **AT1G07890** (APX1) -cw, cl, cls, cyt, mem, pd		
	ath00500 Starch and sucrose metabolism	(2) **AT2G40840** - cyt AT3G29320 (PHS1) – cl, cls, pl		(2) AT1G47840 (HXK3) - cl AT3G25140 (GAUT8) – mit, gol	(1) AT1G23190 (PGM) – cl, nuc, mem, cyt, cp
	ath00620 Pyruvate metabolism	(5) **AT1G01090** – cl,cle,cls,pl **AT1G54220** - mit **AT3G17240** (E3)– cl,mit,mitx **AT3G22960** (PKP-Alpha) – cl,cls **AT5G09660** – ap, cl, cle, mib, px, vac		(1) **AT3G47520** (MDH) – ap, cl, cle, cls, mem, vac, mit	
	ath00630 Glyoxylate and dicarboxylate metabolism	(1) **AT5G09660** – ap, cl, cle, mib, px, vac		(1) **AT3G47520** (MDH) – ap, cl, cle, cls, mem, vac, mit	(1) AT2G44350 (ATCS) – cw, cl, mit
	ath00650 Butanoate metabolism	(1) **AT1G01090** – cl,cle,cls,pl			(2) AT4G11820 (MVA1) – cyt, pd AT5G17330 (GAD) - cyt
Energy metabolism		(8)	(3)	(3)	(1)
	ath00190 Oxidative	(1) AT2G07698 – cl, cle, mem,		(1) **AT5G13450** (ATP5) - mit	(1) **AT5G08690** – cle, mit, nuc

	phosphorylation	mit, nuc, vac			
	ath00710 Carbon fixation in photosynthetic organisms	(5) **AT3G12780** (PGK1) -all AT3G22960 (PKP-Alpha) – cl,cls AT3G52930 (FBA) - all AT4G38970 (FBA2) – cl,cle,cls,mem,ap,thy,plg **AT5G09660** – ap, cl, cle, mib, px, vac	(2) **AT1G23310** (GGT1) -ap, cl, mem, px, vac **AT5G11520** (ASP3) – mem, px, pl	(1) **AT3G47520** (MDH) – ap, cl, cle, cls, mem, vac, mit	
	ath00920 Sulfur metabolism	(2) **AT3G61440** (ATCYSC1) – cl, mit **AT4G14880** (OASA1) - all	(1) AT3G22890 (APS1) – cl, cls, mem	(1) **AT4G14880** (OASA1) - all	
Amino acid metabolism		(9)	(8)	(4)	(2)
	ath00250 Alanine, aspartate and glutamate metabolism		(2) **AT1G23310** (GGT1) -ap, cl, mem, px, vac **AT5G11520** (ASP3) – mem, px, pl		(1) AT5G17330 (GAD) - cyt
	ath00260 Glycine, serine and threonine metabolism	(3) **AT3G17240** (mtLPD2) – cl,mit,mitx AT4G33010 – ap, cl, cle, cls, thy, mit AT4G34200 – cl, cls, mem, mit			
	ath00270 Cysteine and methionine metabolism	(2) **AT3G61440** (ATCYSC1) – cl, mit **AT4G14880** (OASA1) - all	(2) AT3G17390 (MTO3) – cw, mem, nuc, pd **AT5G11520** (ASP3) – mem, px, pl	(4) **AT1G62380** (ACO2) – cw, cyt, mem, pd AT2G36880 (MAT3) – cyt, mem, pd **AT4G14880** (OASA1) - all AT5G17920 (ATMS1) – all except nuc	
	ath00280 Valine, leucine	(1) **AT3G17240** (E3) –			(1) AT4G11820 (MVA1) – cyt,

	and isoleucine degradation	cl,mit,mitx			pd
	ath00290 Valine, leucine and isoleucine biosynthesis	(1) **AT1G01090** – cl,cle,cls,pl			
	ath00330 Arginine and proline metabolism	(1) AT1G80600 (WIN1) – cl, cls	(1) **AT5G11520** (ASP3) – mem, px, pl		
	ath00340 Histidine metabolism	(1) AT1G58080 – cl, cls			
	ath00350 Tyrosine metabolism		(1) **AT5G11520** (ASP3) – mem, px, pl		
	ath00360 Phenylalanine metabolism		(1) **AT5G11520** (ASP3) – mem, px, pl		
	ath00400 Phenylalanine, tyrosine and tryptophan biosynthesis		(1) **AT5G11520** (ASP3) – mem, px, pl		
Other		(14)	(9)	(14)	(17)
	ath00970 Aminoacyl-tRNA biosynthesis	(2) AT3G48110 – cl, cls, mit AT5G52520 (OVA6) – cl, cls, mit			
	ath00230 Purine metabolism	(2) **AT3G22960** (PKP-Alpha) – cl,cls AT5G35170	(2) AT1G63660 – cyt AT3G22890 (APS1) – cl, cls, mem		(2) AT1G23190 (PGM) – cl, nuc, mem, cyt, cp **AT3G55010** (FGAM) – cl, cls, mit
	ath00860 Porphyrin and chlorophyll	(2) AT3G48730 – cl, cls, cle AT5G45930– cl, cls	(1) AT5G63570 (GSA1) – ap, cl, cls, cle		

metabolism				
ath00480 Glutathione metabolism	(2) AT1G65930 (clCDH) – ap, cls, cyt, pd, mem AT2G47730 (GST6) – cl, cle, cls, nuc, thy, mem	(2) **AT1G07890** (APX1) -cw, cl, cls, cyt, mem, pd AT3G02360 – cls, cyt, px		(2) AT4G29210 (GGT3) - vac
Ath04626 Plant-pathogen interaction	(1) AT4G20360 (ATRABE1B) – (all except cyt)	(1) AT4G20360 (ATRABE1B) – (all except cyt)		
ath00061 Fatty acid biosynthesis	(1) AT2G30200– cl, cls			
ath00944 Flavone and flavonol biosynthesis	(1) AT5G54160 (OMT1) – cyt, nuc, mem, pd			
ath03050 Proteasome	(1) **AT4G38630** (RPN10) – pr, cyt, mem, nuc		(1) AT5G23540 (26S) – pr, cyt, nuc	(2) AT1G56450 (PBG1) – cyt, pr AT1G77440 (PBC2) - pr
ath00460 Cyanoamino acid metabolism	(1) **AT3G61440** (ATCYSC1) – cl, mit			(1) AT4G29210 (GGT3)- vac
ath04146 Peroxisome	(1) AT1G65930 (clCDH) – ap, cls, cyt, pd, mem			
ath00450 Selenocompound metabolism		(1) AT3G22890 (APS1) – cl, cls, mem	(1) AT5G17920 (ATMS1) – all except nuc	
ath00950 Isoquinoline alkaloid biosynthesis		(1) **AT5G11520** (ASP3) – mem, px, pl		
ath00960 Tropane, piperidine and pyridine		(1) **AT5G11520** (ASP3) – mem, px, pl		

alkaloid biosynthesis				
ath03013 RNA transport			(4) **AT1G10840** (3H1) - cyt AT1G49760 (PAB8) - cyt **AT5G20020** (RAN2) – cyt, cp, nuc AT5G60390 (EF1-alpha) – cp, mit, nuc, vac, mem, pd	
ath00520 Amino sugar and nucleotide sugar metabolism			(2) AT1G47840 (HXK3) - cl AT3G25140 (GAUT8) – mit, gol	(1) AT1G23190 (PGM) – cl, nuc, mem, cyt, cp
ath04141 Protein processing in endoplasmic reticulum			(1) AT1G16190 (RAD23) – nuc, pr	(1) **AT5G42020** (BiP) – er, mem, vac, cw, pd
ath03420 Nucleotide excision repair			(1) AT1G16190 (RAD23) – nuc, pr	
ath03015 mRNA surveillance pathway			(1) AT1G49760 (PAB8) - cyt	
ath03008 Ribosome biogenesis			(1) **AT5G20020** (RAN2) – cp, nuc	
ath03018 RNA degradation			(1) AT1G49760 (PAB8) - cyt	(1) **AT1G74030** (ENO1) – cl, cls
ath00640 Propanoate metabolism			(1) AT5G08300 – cw, mit	
ath00430 Taurine and hypotaurine				(2) AT4G29210 (GGT3) - vac AT5G17330 (GAD) - cyt

	metabolism				
	ath00900 Terpenoid backbone biosynthesis				(1) AT4G11820 (MVA1) – cyt, pd
	ath03060 Protein export				(1) **AT5G42020** (BiP) – er, mem, vac, cw, pd
	ath00410 beta-Alanine metabolism				(1) AT5G17330 (GAD) - cyt
	ath00072 Synthesis and degradation of ketone bodies				(1) AT4G11820 (MVA1) – cyt, pd
	ath00590 Arachidonic acid metabolism				(1) AT4G29210 (GGT3) - vac

Supplemental Table 3. ABA-related proteins identified as BAP-regulated in the shoot and root. The biological function of each protein and its relation to ABA were obtained from the TAIR database (www.arabidopsis.org), specifically from the "Description" field and from the references cited there.

PROTEIN	TAIR ANNOTATION AND FURTHER REFERENCES
SHOOT	
ATCG00490 (RBCL) 30' up, 120' down	Large subunit of RUBISCO. It is tyrosine-phosphorylated and its phosphorylation state is modulated in response to ABA in *Arabidopsis thaliana* seeds (TAIR description).
AT1G23310 (GGT1) 30' down	Protein with glyoxylate aminotransferase activity. Localized to the peroxisome and thought to be involved in photorespiration/metabolic salvage pathway (TAIR description). The *ggt1-1* mutant shows a reduction in ABA-responsive RD29A expression and, in the absence of ABA treatment, root elongation of ggt1-1 was reduced nearly 50% compared to wt (Verslues et al., 2007).
AT4G14880 (OASA1) 30' up	Encodes a cytosolic isoform of cytosolic O-acetylserine(thiol)lyase, a key enzyme in cysteine biosynthesis and for the fixation of inorganic sulfide. It catalyzes the formation of cysteine from O-acetylserine and inorganic sulfide. Gene expression is predominant in the root cortex and the xylem parenchyma. Gene expression is induced in leave, stems and roots by high salt and heavy metal stresses, mediated by ABA. Lines carrying semi-dominant mutations exhibit early senescence (TAIR description).
AT4G38970 (FBA2) 30' up	Protein is tyrosine-phosphorylated and its phosphorylation state is modulated in response to ABA in *Arabidopsis thaliana* seeds (TAIR description).
AT4G28520 (CRU3) 30' up	Encodes a 12S seed storage protein that is tyrosine-phosphorylated and its phosphorylation state is modulated in response to ABA in *Arabidopsis thaliana* seeds (TAIR description).
AT4G38630 (RPN10) 120' up	Regulatory particle non-ATPase subunit of the 26S proteasome with multiubiquitin-chain-binding capabilities (TAIR description). The *rpn10-1* mutant has a reduced germination rate, increased rosette leaf senescence, a reduction in stamen number, increased sensitivity to DNA damaging agents, decreased sensitivity to cytokinin, and increased sensitivity to abscisic acid, sucrose, and salt (Smalle et al., 2003), providing thus additional evidence of crosstalk between ABA and CK by means of RPN10.
ROOT	
AT2G21660 (CCR2/GRP7) 120' up	Encodes a small glycine-rich RNA binding protein that is part of a negative-feedback loop through which AtGRP7 regulates the circadian oscillations of its own transcript. Gene expression is

	induced by cold. GRP7 appears to promote stomatal opening and reduce tolerance under salt and dehydration stress conditions, but, promotes stomatal closing and thereby increases stress tolerance under conditions of cold tolerance. Loss of function mutations have increased susceptibility to pathogens suggesting a role in mediating innate immune response. Mutants are also late flowering in a non-photoperiodic manner and are responsive to vernalization suggesting an interaction with the autonomous flowering pathway. There is a reduction of mRNA export from the nucleus in grp7 mutants. GRP7:GFP fusion proteins can be found in the cytosol and nucleus. A substrate of the type III effector HopU1 (mono-ADP-ribosyltransferase) (TAIR description). ABA-induced stomatal closure is decreased, cold-induced stomatal opening is increased, and NaCl and mannitol-induced stomatal closing is increased in grp7-KO plants relative to wild type (Kim et al., 2008).
AT4G14880 (OASA1) 120' up	Encodes a cytosolic isoform of cytosolic O-acetylserine(thiol)lyase, a key enzyme in cysteine biosynthesis and for the fixation of inorganic sulfide. It catalyzes the formation of cysteine from O-acetylserine and inorganic sulfide. Gene expression is predominant in the root cortex and the xylem parenchyma. Gene expression is induced in leave, stems and roots by high salt and heavy metal stresses, mediated by ABA. Lines carrying semi-dominant mutations exhibit early senescence (TAIR description).

Supplemental Table 4. Overlay of proteins identified in our study with the ethylene-mediated proteome response in the whole seedling as identified by Chen et al. Out of 8 proteins identified in both studies, 5 were identified to be CK-regulated in the root and all of these show the same type of regulation as identified for ethylene. 30' up/down denotes proteins up-/downregulated, respectively after 30 min, while 120' up/down denotes proteins up-/downregulated after 120 min. S/R indicates proteins identified in the shoot/root while up/down stands for protein up-/downregulated.

AGI code	**Name**	**Zdarska et al.**	**Chen et al., 2011**
AT3G25140	GAUT8 (galacturonosyltransverase 8)	120' R, up	up
AT1G29670	GDSL-motif lipase/hydrolase family protein	120' S, down	up
AT1G10840	eukaryotic initiation factor 3H1 subunit	30' R, up	up
AT3G16460	T2O44 (mannose-binding lectin superfamily protein)	30' R, down	down
AT5G23540	Mov34/MPN/PAD-1 family protein - 26S proteasome regulatory subunit, putative (26S)	120' R, up	up
AT5G42020	BiP (luminal binding protein)	120' R, down	down
AT4G20360	ATRABE1B (Arabidopsis Rab GTPase homolog E1b)	30' S, up 120' S, down	up
AT1G30580	GTP binding	30' S, down	up

Supplemental Materials and Methods

LC–MS/MS analysis and MS Data Processing. Prior to LC separation, tryptic digests were concentrated and desalted using trapping column (100 µm × 30 mm) filled with 4-µm Jupiter Proteo sorbent (Phenomenex, Torrance, CA). Sample volume was 10 µl. After washing with 0.1% formic acid, the peptides were eluted from the trapping column using an acetonitrile/water gradient (350 nL/min) onto a fused-silica capillary column (100 µm x 100 mm), on which peptides were separated. The column was filled with 3.5-µm X-Bridge BEH 130 C18 sorbent (Waters, Milford, MA, USA). The mobile phase A consisted of 0.1% formic acid in water and the mobile phase B consisted of 0.1% formic acid in acetonitrile. The gradient elution started at 10 % of mobile phase B and increased linearly from 10 % to 30 % during the first 10 minutes. The gradient linearly increased to 90 % of mobile phase B in the next two minutes and remained at this state for next 8 minutes. Equilibration of the precolumn and the column was done prior to sample injection to sample loop. The analytical column outlet was directly connected to the nanoelectrospray ion source. Nitrogen was used as nebulizing as well as drying gas. The pressure of nebulizing gas was 8 psi. The temperature and flow rate of drying gas were set to 250 ºC and 6 L/min, respectively, and the capillary voltage was 4.0 kV.

The mass spectrometer was operated in the positive ion mode in m/z range of 300 – 1500 for MS and 100-2500 for MS/MS scans. Two precursor ions per mass spectrum were selected in data dependent manner for further fragmentation. Extraction of the mass spectra from the chromatograms, mass annotation and deconvolution of the mass spectra were performed using DataAnalysis 4.0 software (Bruker Daltonik).

MASCOT 2.2 (MatrixScience, London, UK) search engine was used for processing the MS and MS/MS data. Database searches were done against the NCBI database (non redundant, taxonomy *Arabidopsis thaliana*; downloaded from ftp://ftp.ncbi.nih.gov/blast/db/FASTA/). Database was updated regularly. Mass tolerances of peptides and MS/MS fragments for MS/MS ion searches were 0.5 Da. Oxidation of methionine and carbamidomethylation of cysteine as optional modifications, one enzyme miscleavage and correction for one ^{13}C atom were set for all searches. Quality of the protein identifications was checked manually via examination of MASCOT

results of the corresponding peptides. Out of the spots subjected to digestion and LC-MS/MS analysis, 87 % of spots from the shoot and 94 % of spots from the root yielded positive identification result with at least one peptide with significant MASCOT score ($p < 0.05$; peptide MASCOT score 45 or higher). In the result list, protein identifications based on two or more peptides with significant MASCOT score are distinguished from those based on single peptide with significant MASCOT score (see Suppl. Table 1).

The **Western immunoblotting** of AtPHB3 protein was performed with extra protein isolation and entire 2DE gels procedure of root samples treated with BAP/mock for 2 hours. We applied approx. 50 micrograms whole protein sample in 125 µL IPG buffer per IPG strip was applied to 7 cm ReadyStrip IPG strips pH 3–10NL (Bio-Rad) and in the second dimension we used 12% SDS-PAGE gels again that ran in Mini-Protean 3 Dodeca Cell (Bio-Rad). Separated proteins were then transferred overnight to polyvinylidene difluoride membrane (PVDF, MERCK-Millipore, IPVH 00010 pore size 0.45 µm) at 40 V. As a blocking buffer was employed 5% (w/w) non-fat dry milk in TBST and protein was detected with polyclonal antibody against Arabidopsis prohibitin (Snedden and Fromm, 1997; 1:2000) and anti-rabbit IgG-Alkaline phosphatase (Sigma; 1:20 000). The protein quantification was evaluated in Quantity One 4.6.1 software (Bio-Rad) using volume tools. The rabbit polyclonal antibody to histone H3A (Abcam; 1:2000). was used as an internal control for protein amount normalization and its relative quantification.

Protein mapping. Proteins identified in the study were mapped using the *Arabidopsis thaliana* KEGG Pathway tool [(Ogata et al., 1999), http://www.genome.jp/kegg-bin/show_organism?org=ath]. These maps allow visualizing the potential role of the proteins in particular cellular processes (Supplemental Figures 2 and 3). The mapping data were integrated into Supplemental Table 2, which was complemented with the information for intracellular localization and biological activity available in the TAIR database.

Measurement of ABA. Accurately weighted plant material (around 0.5 g FW) was ground to powder in liquid nitrogen and extracted overnight by 3 ml (3 times) of modified

Bieleski solution. The extract was centrifuged and purified by using SPE method. For that, solid phase extraction (SPE) column C_{18} (Strata C18-T, 55 µm, 140A, 500 mg/6 mL; Alltech, U.S.A.) was conditioned by 10 ml of methanol and 10 ml of water; thereafter the extract was applied on column to dispose of non – polar compounds. The eluate was partly evaporated by the rotary vacuum evaporator (RVE) to end volume of approx. 3 ml. The pH was then adjusted by 1 ml of 1 M formic acid. The adjusted eluate was applied on the MCX SPE column (Oasis, MCX 6cc 150 mg; Waters, U.S.A.), cleaned by 2 ml of 1 M formic acid, eluted by 5 ml of 100% methanol and dried on the rotary vacuum concentrator.

Dried samples were diluted in 15 % (v/v acetonitrile:water) solution and filtered on Nylon 0.2 µm Micro-Spin filters. Filtrates were injected to HPLC (Agilent 1200, U.S.A.) equipped with UV-detector at 270 nm, and precleaned on C-18 column (Luna 3 µm 150x4, 60 mm, Phenomenex, U.S.A.) with gradient elution and fractionated on a fraction collector (Gilson 203B, Middleton, WI, U.S.A.).

Gradient:

Time (min)	A: Water	B: Acetonitrile	C: HCOOH 1%	Flow ($ml.min^{-1}$)
0	70	10	20	0.6
15	60	20	20	0.6
30	0	90	10	0.6
45	70	10	20	1.0
50	70	10	20	0.6

Fraction at time 23.05 min was collected for 1 min and dried. After drying collected fraction was derivatized by 0.3 ml diazomethane for 15 min, dried, dissolved in 10 µl of acetone. 8 µl of redissolved sample were injected into GC-MS/MS (PolarisQ, ThermoFisher Scientific, Waltham, MA, U.S.A.) and analyzed on column DB-5MS under these conditions: injector - programmable temperature vaporizer in solvent split mode, 8 µl injection; oven – $60^{o}C$ (hold 3.5 min), $60^{o}C.min^{-1}$ to$160^{o}C$ (hold 0 min), $8^{o}C.min^{-1}$ to

250^{o}C (hold 5 min); flow: He 1.5 ml.min^{-1}; detector: Ion trap in MS/MS scan mode (MS1: full scan 50-300 amu; MS2 IAA: precursor 130.1 amu, product full scan 65-200 amu; MS2 labeled IAA: precursor 136.1 amu, product full scan 70-200 amu; MS2 ABA: precursor 190.2 amu, product full scan 65-200 amu; MS2 labeled ABA: precursor 194.2 amu, product full scan 70-200 amu).

Measurement of ACC. Accurately weighted plant material (around 0.2 g FW) was ground to powder in liquid nitrogen and extracted overnight by 3 ml (3 times) of 80% (v/v) methanol. The extract was centrifuged and purified by using SPE method. For that, SPE column C_{18} (Strata C18-T, 55 µm, 140A, 500 mg/6 mL; Alltech, U.S.A.) was conditioned by 10 ml of methanol and 10 ml of water; thereafter the extract was applied on column to dispose of non – polar compounds. The eluate was partly evaporated by the rotary vacuum evaporator (RVE) to end volume of approx. 3 ml. The pH was then adjusted to 2 by 0,1 M hydrochloric acid. The adjusted eluate was applied on the SCX SPE column (Extract Clean, SCX 200 mg; Grace, U.S.A.), cleaned by 2 ml of deionized water, eluted by 3 ml of 4M Ammonium hydroxide solution and dried on the rotary vacuum concentrator.

After drying sample was derivatized by 4 µl 2, 3, 4, 5, 6-Pentafluorobenzyl bromide for 15 min, dried, dissolved in 200 µl of hexane and cleaned by liqud-liqud extraction with 500 µl of deionized water. Hexane layer was dried and redissolved to 50 µl of hexane. 5 µl of redissolved sample were injected into GC-MS/MS (PolarisQ, ThermoFisher Scientific, Waltham, MA, U.S.A.) and analyzed on column DB-5MS under these conditions: injector - programmable temperature vaporizer in solvent split mode, 5 µl injection; oven – 50^{o}C (hold 1 min), 10^{o}C.min^{-1} to 250^{o}C (hold 5 min); flow: He 1.5 ml.min^{-1}; detector: Ion trap in CI - MS/MS scan mode (MS1: full scan 150-400 amu; MS2 ACC: precursor 280.1 amu, product full scan 150-300 amu; MS2 labeled ACC: precursor 284.1 amu, product full scan 150-300 amu).

qRT-PCR and data analysis. Total RNA from plant tissue was isolated using the RNAqueous Small Scale Phenol-Free Total RNA Isolation Kit (Ambion) according to the manufacturer's instructions. cDNA was prepared using RTP3 primer and Superscript III (Invitrogen) according to the manufacturer's instructions, and qRT-PCR was performed

using the DyNAmo Flash SYBR Green qPCR Kit (Finnzymes) according to the manufacturer's instructions on a Rotor-Gene 3000 (CORBETT RESEARCH) instrument.

RTP3 primer: 5´ CGT TCG ACG GTA CCT ACG TTT TTT TTT TTT TTT TT 3´

For comparison of proteomic response of 20 proteins with their transcriptional regulations we used following primers:

fTON1rt (5'-TAACAAGAGCTTCAGCGG-3')

rTON1 rt (5'-CCATCCCTCACATTCCTC-3')

fPBC2 rt (5'-TTCTCTCTTCAGTTGACCG-3')

rPBC2 rt (5'-TCTCCTTCACCTCCTTTG-3')

fCCRfamily rt (5'-GGTCCGATCTTGATTTTTG-3')

rCCRfamily rt (5'-GTTGGTTCCATGCTTCTCC-3')

f26S rt (5'-TGACACCCACTCCAAGACC-3')

r26S rt (5'-CGCCTTGTTATATTTAGCAGCC-3')

fATMS1 rt (5'-GCTTTCTACTTGGACTGGG-3')

rATMS1 rt (5'-TGATGTCATTGAAGTGGGA-3')

fBiP rt (5'-CCGTCTCCATTCAGGTCTTT-3')

rBiP rt (5'-CGCCTTGTCCTCTGCTTTC-3')

fACO2 rt (5'-GCAGGAGGCATCATCTTG-3')

rACO2 rt (5'-ACCGACATCCTGTTTCCTTC-3')

fCCR2 rt (5'-CGGTGCTTCGTTGGAGGT-3')

rCCR2 rt (5'-CGAATCCGAATCCCCTTGA-3')

fATPHB3 rt (5'-ATCCGCACGAAGCCTCAC-3')

rATPHB3 rt (5’-TCAGGACGAGAGAGAACACG-3’)AA

fAXR1 rt (5’-CGATTAAAAACTACTGCCTTGA-3’)

rAXR1 rt (5’-AGATGCGATTCCTCCAAC-3’)

fOMT1 rt (5’-AAGTGTCCCTAAAGGTGATG-3’)

rOMT1 rt (5’-GAGGCTTGAGTCTGGTGT-3’)

fOVA6 rt (5’-CGAGGAGGGATGTACCAGGA-3’)

rOVA6 rt (5’-AAGGACCTCTTGCCCATTTC-3’)

fEDA9 rt (5’-CATGGAGGCTCAGGAAGGA-3’)

rEDA9 rt (5’-TGGTTTCAGCTCGGTCAGA-3’)

fMAT4 rt (5’-GATTGTGAAGGAGAGTTTTGA-3’)

rMAT4 rt (5’-AGTGACCATAGGCAGCAG-3’)

fFBA2 rt (5’-TCCTCCGCAACAGAGTCC-3’)

rFBA2 rt (5’-GGTTTGGTGCCTGGTTCA-3’)

fOASA1 rt (5’-GCTGGGAAGCTATTTGTG-3’)

rOASA1 rt (5’-CTTCTTTCCTTGTCGCATC-3’)

fRPN10 rt (5’-CTGTTCTCTCATCGCTTCCT-3’)

rRPN10 rt (5’-GCTTTGACTCGTCTGGCA-3’)

fCRU3 rt (5’-ATCTTGGAGTATGTCAGGCT-3’)

rCRU3 rt (5’-GCGTTCATGTTGTATTTAGG-3’)

fGST6 rt (5’-ACGGTGATTTGACGCTTT-3’)

rGST6rt (5’-CGTTAGTGGTTGCCTTG-3’)

fAKR2 rt (5’-GGTTACGGGAGGAAAGAG-3’)TG

rAKR2 rt (5’-GGCTGTTGAGCTTCGCTA-3’)

For individual pairs of primers we used following conditions:

TON1, PBC2, CCRfamily, 26S, ATMS1, BiP, ACO2, CCR2, ATPHB3, OVA6, EDA9, FBA2 , OASA1, RPN10, CRU3, AKR2: 95 °C/7 min – 35x (95 °C/15 s + 60 °C/20 s + 72 °C/20 s) – 72 °C/1 min – melt

AXR1: 95 °C/7 min – 35x (95 °C/15 s + 62 °C/20 s + 72 °C/11 s) – 72 °C/1 min – melt

OMT1: 95 °C/7 min – 35x (95 °C/15 s + 60 °C/20 s + 72 °C/13 s) – 72 °C/1 min – melt

MAT4: 95 °C/7 min – 35x (95 °C/15 s + 62 °C/20 s+72 °C/18 s) – 72 °C/1 min – melt

GST6: 95 °C/7 min – 35x (95 °C/15 s + 62 °C/20 s+72 °C/18 s) – 72 °C/1 min – melt

All expression levels were normalized to *UBIQUITIN10 (Q10)* as described (Pernisova et al., 2009).

Calculation of relative level of gene expression. First, all expression levels (Ct values) were normalized to reference gene *Q10* to obtain dCt value and relative gene expression (RQ) was calculated using formula RQ = 2 exp - (dCt). RQ values were log transformed prior statistical analysis because qRT-PCR data are typically non-linearly distributed across biological replicates (Rieu and Powers, 2009). For the evaluation of statistical significance we used t test at=alpha 0.05, 0.01, and 0.001 that is in figures denoted by *, **, and ***, respectively.

Supplemental References

Chen R, Binder BM, Garrett WM, Tucker ML, Chang C, Cooper B (2011) Proteomic responses in Arabidopsis thaliana seedlings treated with ethylene. Mol Biosyst

Kim K, Ryu H, Cho YH, Scacchi E, Sabatini S, Hwang I (2011) Cytokinin-facilitated proteolysis of ARABIDOPSIS RESPONSE REGULATOR 2 attenuates signaling output in two-component circuitry. Plant J

Ogata H, Goto S, Sato K, Fujibuchi W, Bono H, Kanehisa M (1999) KEGG: Kyoto Encyclopedia of Genes and Genomes. Nucleic Acids Res

Rieu I, and Powers SJ (2009) Real-time quantitative RT-PCR: design, calculations, and statistics. Plant Cell

Smalle J, Kurepa J, Yang P, Emborg TJ, Babiychuk E, Kushnir S, Vierstra RD (2003) The pleiotropic role of the 26S proteasome subunit RPN10 in Arabidopsis growth and development supports a substrate-specific function in abscisic acid signaling. Plant Cell **15:** 965-980

Snedden WA, Fromm H (1997) Characterization of the plant homologue of prohibitin, a gene associated with antiproliferative activity in mammalian cells. Plant Mol Biol **33:** 753-756

Tran LS, Urao T, Qin F, Maruyama K, Kakimoto T, Shinozaki K, Yamaguchi-Shinozaki K (2007) Functional analysis of AHK1/ATHK1 and cytokinin receptor histidine kinases in response to abscisic acid, drought, and salt stress in Arabidopsis. Proc Natl Acad Sci U S A

Verslues PE, Kim YS, Zhu JK (2007) Altered ABA, proline and hydrogen peroxide in an Arabidopsis glutamate:glyoxylate aminotransferase mutant. Plant Mol Biol